2
3-21-77

ORNL/Sub/3670-5

MASTER

THE MINERALOGY, PETROLOGY AND BROMINE GEOCHEMISTRY OF SELECTED SAMPLES OF THE SALADO SALT, LEA AND EDDY COUNTIES, NEW MEXICO - A POTENTIAL HORIZON FOR THE DISPOSAL OF RADIOACTIVE WASTE

Douglas W. Combs

December 1975

This report was prepared by D. W. Combs under the provisions of Subcontract 3670 between the University of Tennessee and Union Carbide Corporation, Nuclear Division. The subcontract was administered by Oak Ridge National Laboratory.

prepared for the **U.S. ENERGY RESEARCH AND DEVELOPMENT ADMINISTRATION**
under **U.S. GOVERNMENT** *Contract W-7405 eng 26*

THE MINERALOGY, PETROLOGY AND BROMINE GEOCHEMISTRY OF SELECTED SAMPLES OF THE SALADO SALT, LEA AND EDDY COUNTIES, NEW MEXICO—A POTENTIAL HORIZON FOR THE DISPOSAL OF RADIOACTIVE WASTE

A Thesis

Presented for the

Master of Science

Degree

The University of Tennessee

Douglas W. Combs

December 1975

ACKNOWLEDGMENTS

The author would like to express his appreciation to the Union Carbide Nuclear Corporation, Oak Ridge, Tennessee for the funding of this research. I wish to thank Mr. Don Schlafke of ORTEC, Oak Ridge, Tennessee, for his technical assistance and permitting me to use the ORTEC-TEFA 6110 Spectrograph for my bromine analyses. I would like to express my sincere appreciation to my advisor, Dr. O. C. Kopp not only for his thorough guidance of this thesis but for being a concerned teacher, as well. In addition, I wish to thank Dr. H. J. Klepser and Dr. J. H. Rule for their helpful comments during the preparation of this manuscript.

ABSTRACT

The main purpose of this study was to evaluate the mineralogy, petrology and dehydration characteristics of the Salado Salt near Carlsbad, New Mexico which is a potential radioactive waste (radwaste) repository. Bedded evaporite deposits were previously selected by the National Academy of Sciences-National Research Council because of their general lack of water, self-healing property when fractured, thermal conductivity and stopping power of high energy radiation. The Salado Salt was chosen using these guidelines. It is a bedded evaporite sequence (about two-thousand feet thick) of late Permian age located in southeastern New Mexico and west Texas. The Salado is composed primarily of halite with lesser amounts of anhydrite, polyhalite and with a zone of economic potash minerals (McNutt potash zone).

Several techniques were employed in this study. X-ray diffraction was used to determine the bulk mineralogy and relative amount of each mineral. Thin section analyses were used to study the mineral assemblages, textures and paragenesis. Non-dispersive X-ray spectroscopy was used to analyze the bromine content of each sample and to give insight into the origin of the Salado. Samples from a previous study of the Hutchinson Salt Member (lower Permian) of the Wellington Formation (near Lyons, Kansas) were also analyzed for bromine in order that a comparison could be made between two deposits of Permian age. Static dehydration tests made of each sample to estimate the amount of water that would be released when subjected to heat of decaying

radioactive waste were reported separately in the Final Report for this project (Kopp and Combs, 1975).

Samples were prepared for thin-sectioning by cutting a slab from each core section and sending it away to be made using oil during cutting and grinding, rather than water. Also the epoxy cement was not heated. These steps were necessary to prevent dissolution and/or changes of the evaporite minerals.

Pressed-pellets were made for spectroscopic analysis of bromine, chlorine, sulfur and iron using clear, cubic halite crystals with a minimum of inclusions. This procedure was used to be sure that the bromine analyses were only for halite without dilution or addition of bromine from other minerals. Bromine values determined for 73 samples of the Salado Salt ranged from 17 to 50 ppm. Semiquantitative analyses for sulfur and chlorine were run to measure the amount of contamination by sulfates and to insure that relatively equal amounts of chlorine were present. Sulfur contents were roughly less than 10 ppm.

The results of this study show that: (1) halite is the dominant mineral in all but a few samples with anhydrite being next most abundant in the lower portions of the Salado Salt and polyhalite being second most abundant in the upper part of the unit, (2) thin section analyses reveal several shallow-water features such as hopper crystals, halite embedded in clay and nodular anhydrite, (3) polyhalite commonly occurs as a secondary mineral at the expense of anhydrite, (4) both anhydrite and polyhalite exist in various habits and associations, (5) spectroscopic analyses reveal low bromine concentrations for the Salado (and the

Hutchinson Salt, Lyons, Kansas), suggesting that both are second generation deposits, (6) dehydration studies show the Salado to lose 0.0 to 3.5 percent water upon heating to 102 ± 5°C. Most of the higher weight losses (>0.5 percent) can be related to zones rich in clays and/or polyhalite. The Salado is a potential site for a radwaste repository if clay- and polyhalite-rich zones are avoided.

TABLE OF CONTENTS

LIST OF TABLES

LIST OF FIGURES

LIST OF PLATES

CHAPTER I

INTRODUCTION

Which was which he could never make out
In spite of his best endeavor
Of that there is no possible doubt
No probable, possible shadow of doubt
No possible doubt whatever

W. S. Gilbert: The Gondoliers

Purpose of Study

With the greater demand for energy to maintain and improve our present standard of living, nuclear power may well become a more important source of energy for our modern society. However, along with this efficient and economical means of power generation will come problems associated with the disposal of radioactive waste (radwaste) produced. As more and more nuclear power plants replace conventional power producers, greater amounts of both high and low-level radwaste will have to be handled and disposed of safely. Since it takes many years for some radioactive isotopes to decay into harmless daughter elements, a secure environment for waste disposal is essential. In 1957 a committee of the National Academy of Sciences-National Research Council (NAS-NRC) concluded that natural salt deposits would provide such a medium because of their general lack of water, self-healing property when fractured, thermal conductivity and stopping power of high energy radiation. Subsequent reviews in 1961, 1966 and again in 1970 by NAS supported the idea that bedded salt deposits would be the

most promising terrestrial location for the disposal of radwaste. One of the recently chosen sites for a potential radwaste repository is located approximately 30 miles (45 km) east of Carlsbad, New Mexico (Figure 1).

The primary purpose of this study was to determine whether there are any water-bearing minerals present at the proposed site which might dehydrate when subjected to radioactive heating, thereby producing a potential source of hazardous fluids at a later time. The investigation was conducted with the same general methods used in previous studies on the Hutchinson Salt Member of the Wellington Formation near Lyons, Kansas (Fallis, 1973; Kopp and Fallis, 1973). In addition to determining the types and relative quantities of minerals present at the New Mexico repository site, it was thought that additional information might be gained by reexamining the samples from Lyons, Kansas and comparing the results of the data from the two localities. By relating mineralogical, petrological and chemical information for both sites, it was hoped that some insight might be gained concerning the deposition of evaporites in the southwestern United States during Permian time.

Finally, an attempt was made to establish some relationship between the mineralogical and petrologic characteristics and the water loss on heating that would enable future investigators to search more efficiently for potential disposal horizons.

Development of Evaporite Sequences

Superficially, the formation of evaporite sequences appears to be rather simple, however, in spite of much research many questions are

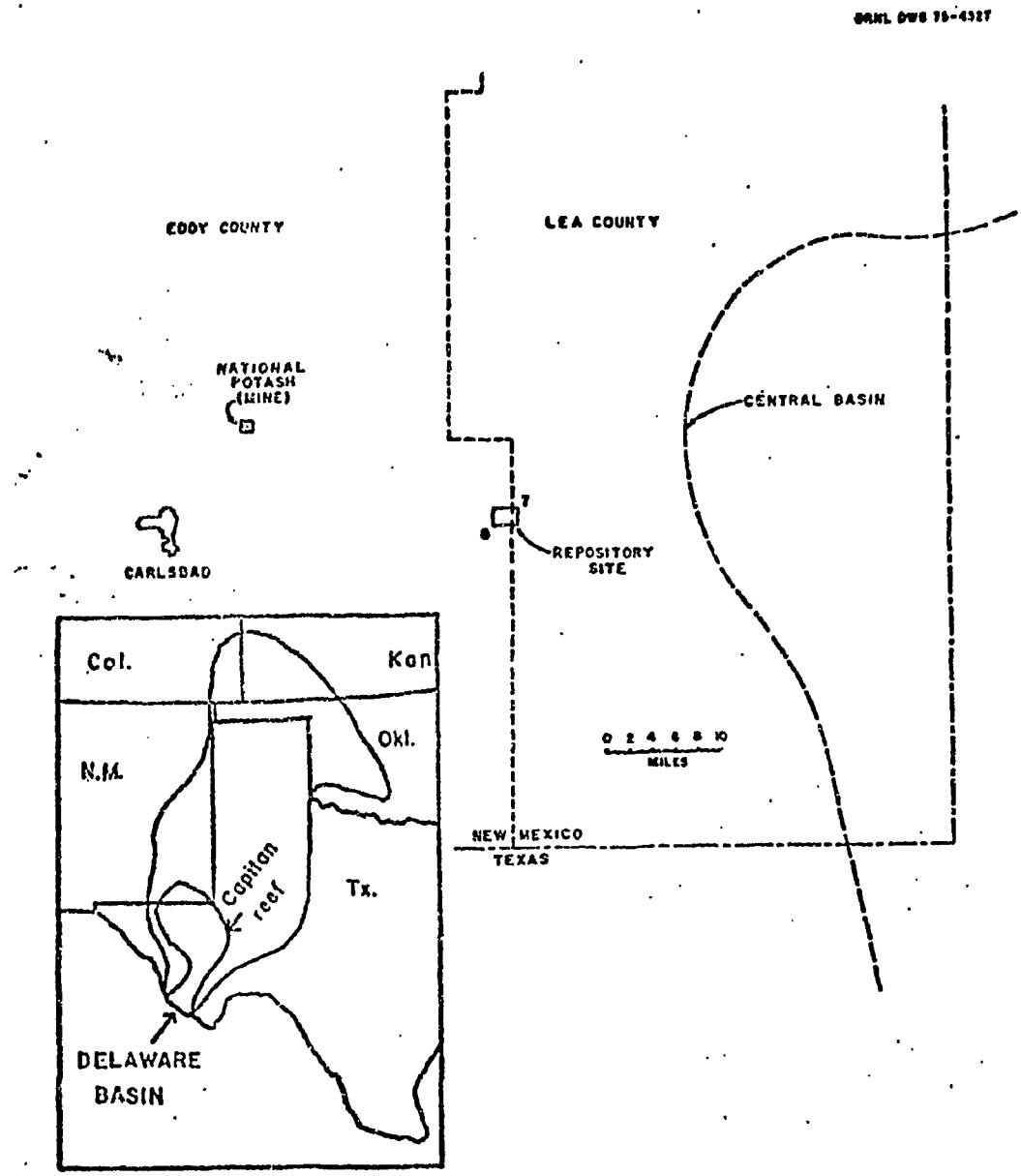

Figure 1. Location of drill cores AEC #7 and #8 in southeast New Mexico.

Insert shows Permian Basin surrounding Delaware Basin.

still unanswered. Braitsch (1971) compiled an extensive treatise on the geochemistry of evaporites. Some workers (Holser, 1966; Valyashko, 1956; Kühn, 1968; Nielsen, 1968) approached the subject by considering the geochemistry of specific trace elements. Other researchers (such as Borchert and Muir, 1964) attempted to solve the problems of evaporite origin by examining their distribution, physicochemical characteristics, metamorphism, etc. Still other workers have speculated on the more general aspects of evaporite deposition, such as Raup's (1970) investigation of brine-mixing and Briggs' and Lucas' (1954) research into the mechanics of Salina Salt deposition in the Michigan basin.

Many anomalies exist which do not fit the models developed by these researchers. A good example concerns the formation of polyhalite. Based on geochemical parameters, polyhalite should occur late and make up little of the entire evaporite sequence. However, it is quite abundant throughout the evaporite suite in several deposits. Likewise, the order of mineral deposition in the Zechstein Salt (Germany) is realistic when compared with experimental data only if one assumes a temperature of over 83°C. However, sediments and fossils adjacent to the salt show no such indication of high temperatures (Krauskopf, 1967, p. 350).

Evaporite deposits form in somewhat the same manner as terrigenous marine sedimentary deposits. Many bedded sequences (such as the Silurian salt of the Great Lakes region and the Permian salt of Kansas and Oklahoma) show primary sedimentary structures such as cross-bedding, mud cracks, shale balls, polygonal patterns and unconformities (Dellwig, 1968). However, unlike normal clastic sediments, most of the material is not

directly deposited from suspension to form an evaporite deposit, but remains in solution as a part of the sea water until favorable conditions cause precipitation. The major process involved is evaporation and the process apparently takes place best in a restricted basin which isolates a body of water from the open sea. In an arid region, evaporation may proceed faster than additional water, with its normal constituents (Table I), can enter the basin. The residual brine becomes more concentrated as the soluble, but nonvolatile, ions are left behind. When enough water has been removed from the basin, the brines become concentrated to the point that precipitation will occur. Depending upon the degree of concentration and to a lesser extent upon the temperature, certain minerals will form. In a normal progression the carbonate minerals (calcite, dolomite, magnesite and in some exposed salt flats, aragonite) start to precipitate first, then $CaSO_4$ (as either gypsum or anhydrite), followed by NaCl.

TABLE I

IONS DISSOLVED IN SEA WATER

Ion	Parts Per Million	Percent of Total Salt
Cl^-	18,980	55.05
Na^+	10,556	30.61
SO_4^{--}	2,649	7.68
Mg^{++}	1,272	3.69
Ca^+	400	1.16
K^+	380	1.10
HCO_3^-	140	0.41
Br^-	65	0.19
$H_2BO_4^{--}$	26	0.07
Sr^{++}	8	0.03

Source: After Krauskopf (1967).

In many evaporite sequences the series ends with the formation of halite, or conditions are such that minerals more soluble than halite are not preserved. When evaporation proceeds well past the point of concentration necessary for the deposition of halite, more "exotic" minerals (K^+ and Mg^{++} salts) begin to form. Historically, the investigation of evaporites began when an Italian chemist, Usiglio, allowed sea water to evaporate at 40°C and observed the sequence of compounds formed (Table II). In this way he generally duplicated the mineral sequence found in the salt deposits at Stassfurt, Germany. The mineral suites of evaporite deposits, however, are far from simple. Brine-mixing, variable climatic changes and the addition of terrigenous matter, all produce different primary mineral assemblages and textural features. Once the deposit has formed, diagenetic changes occur aided by the movement of solutions and mineral phase transformation. Petrologists studying evaporites often refer to these changes as "metamorphism." Since the temperature of tranformation is rather low, it becomes a matter of individual preference whether "metamorphism" or "diagenesis" is the more suitable term (Krauskopf, 1967, p. 348).

Several elements control the physical characteristics (shape, aerial extent and thickness) of an evaporite deposit. The form is controlled by the particular shape of the basin in which the salt is deposited, and most have a roughly circular configuration. The climate directly affects the rate of precipitation as does the amount of sea water inflow which provides the needed materials. When speaking of shallow-water evaporite deposition, crustal subsidence is assumed to make space available for continuing salt accumulation.

TABLE II

USIGLIO'S EXPERIMENT SHOWING THE ORDER OF PRECIPITATION OF SALTS (IN GRAMS) FROM 1 LITER OF SEAWATER AT 40°C

Volume	Fe_2O_3	$CaCO_3$	$CaSO_4$	NaCl	$MgSO_4$	$MgCl_2$	NaBr	KCl
1.000								
0.533	0.0030	0.0642						
0.316		trace						
0.245		trace						
0.190		0.0530	0.5600					
0.1445			0.5620					
0.131			0.1840					
0.112			0.1600					
0.095			0.0508	3.2614	0.0040	0.0078		
0.064			0.1476	9.6500	0.0130	0.0356		
0.039			0.0700	7.8960	0.0262	0.0434	0.0728	
0.0302			0.0144	2.6240	0.0174	0.0150	0.0358	
0.023				2.2720	0.0254	0.0240	0.0518	
0.0162				1.4040	0.5382	0.0274	0.0620	
Total	0.0030	0.1172	1.7488	27.1074	0.6242	0.1532	0.224	
salts in last bittern-				2.5885	1.8545	3.164	0.330	0.534
total solids-	0.0030	0.1172	1.7488	29.6959	2.4787	3.3172	0.5524	0.534

Source: After Clarke (1924).

One of the major controversies in geology today concerns the nature of the environment during the formation of most ancient evaporite deposits. Were they shallow-water basins or deep-water basins?

The shallow-water proponents use the present day examples of Baja, California and the Persian Gulf to support their ideas. Kinsman (1969) reported that sabkhas (exposed supratidal salt flats) could develop over an area 100-200 km wide in a relatively short time (10^5 years) with a shoreline regression of 1-2 meters per year. Proponents of deep-water hypotheses reject the idea that major evaporite deposits formed in this manner because an arid climate would need to be continuous for long periods of time. Even minor climatic changes or influxes of fresh water could redissolve the salt and destroy part of the deposit thereby making the accumulation of several thousand feet of evaporites unlikely. Also, since the rate of salt deposition was estimated to have been as much as 15 cm per year in some areas (Schmalz, 1969) the rate of crustal subsidence would be unrealistic.

The deep-water theorists (Sloss, 1969) propose the concept of stratification of brines of different densities. Evaporation would occur at the surface of a body of water thereby concentrating the salts in the uppermost layer, producing a brine of higher density than the rest of the water. The brine would then sink to the bottom. The process would continue until only a thin layer of average-density water existed at the surface which would be maintained by the inflow of sea water. With this protective layer climatic changes and minor influxes of water would not affect the concentrated brine at depth. Subsequent exposure of the lower

brine periodically by wind or wave action pushing the normal-density layer to one side of the basin could concentrate the lower layers to the point of precipitation.

Salado Salt

The formation of main interest in this study is the Salado Salt of the Ochoan Series of late Permian age. It is located in and surrounding the Delaware basin which occupies a portion of southeastern New Mexico and west Texas (Figure 1, page 3). The Ochoan series consists of three formations; the Castile, the Salado and the Rustler (Figure 2). The Salado is divided into three members. The upper and lower members are relatively free from potash minerals and are 100 to 450 feet thick and 1000 to 1150 feet thick, respectively. The middle member which is known as the McNutt Potash zone (about 370 feet thick) is an important potash deposit which has been mined since the 1930's. One of the interests of others working on this project is that the location of a radwaste repository in this vicinity should not restrict the exploitation of any economic minerals.

The area was chosen as a potential repository site for several reasons: (1) the population in this area is very sparse (from 10 to 25 person per square mile, usually in small pockets), (2) the construction of a repository probably will not be hindered by or restrict residential growth, (3) the lithologic character of the rocks is such that the intergranular porosity and permeability ranges from low to none, and (4) tectonic activity of this area has been negligible and only two minor post-Permian faults are evident in the Delaware basin (Clairborne and Gera, 1974, p. 41).

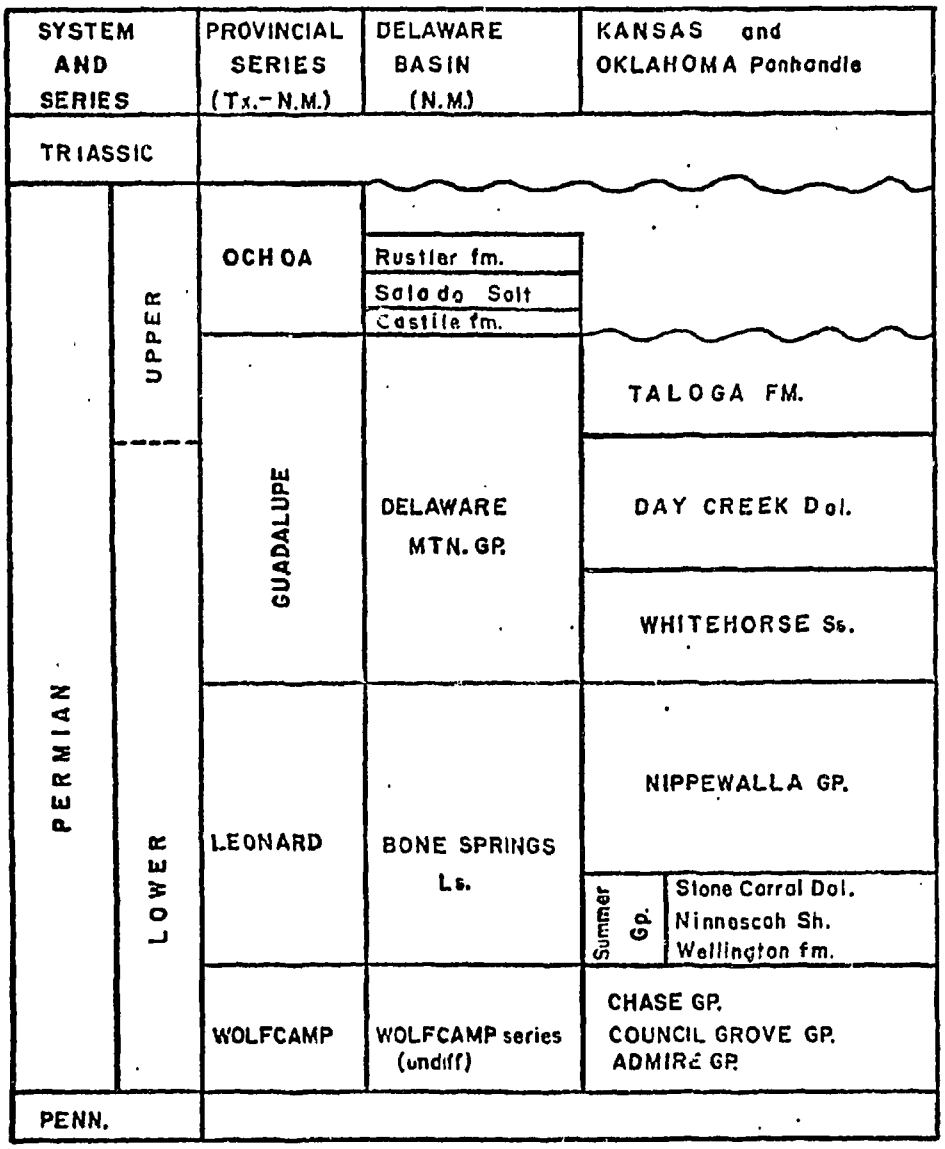

Figure 2. Generalized stratigraphic chart for parts of the Permian basin (after Pierce and Rich, 1962, p. 29).

According to Adams and Frienzel (1950), the depositional history of the Ochoan evaporite sequence began when epicontinental seas covered wide areas of the western and southwestern United States and northern Mexico in the early part of the Permian period. The area became an active geosyncline with subsidence so rapid that the only shallow-water deposits were organic reefs and narrow zones of biostromal limestones on the edge of mountain chains and sea mounts. These early reef structures did not grow fast enough to keep up with the rate of submergence and eventually died out. Later in the period, conditions were favorable for organic growth along the more shallow shelf margins and the Capitan reef began to develop. This reef formed a restricting wall almost completely around the Delaware basin with only one opening to the sea which was the Sheffield Channel to the southwest. During Permian time this restricted basin, with a depth of approximately 1900 feet, proved to be an efficient location for evaporite formation. The basin eventually became filled with finely laminated anhydrite, calcite, halite and dark organics of the underlying Castile Formation of late Permian age. Evaporite precipitation continued and the Salado was deposited over the Castile, northward and eastward over an area of greater extent than just the structural outline of the basin. During the period of wider deposition, potassium-bearing salts were deposited over much of southeastern New Mexico and parts of Texas.

Hutchinson Salt Member of the Wellington Formation

The Hutchinson Salt Member of the Wellington Formation was studied previously (Fallis, 1973; Kopp and Fallis, 1973) and is used here for

comparison purposes with the Salado Salt. It is present in central Kansas (Figure 3), western Oklahoma and part of the Texas panhandle. The Hutchinson of early Permian age (Figure 2, page 10) was deposited at the edge of the Permian basin and consists of carbonates, gypsum, anhydrite, halite and various clastics. The younger part of the Wellington is mostly dark gray shale and the older part consists of anhydrite and gray shale interbedded with dolomite. A detailed mineralogical examination of core samples from the Hutchinson Salt was made by Fallis (1973).

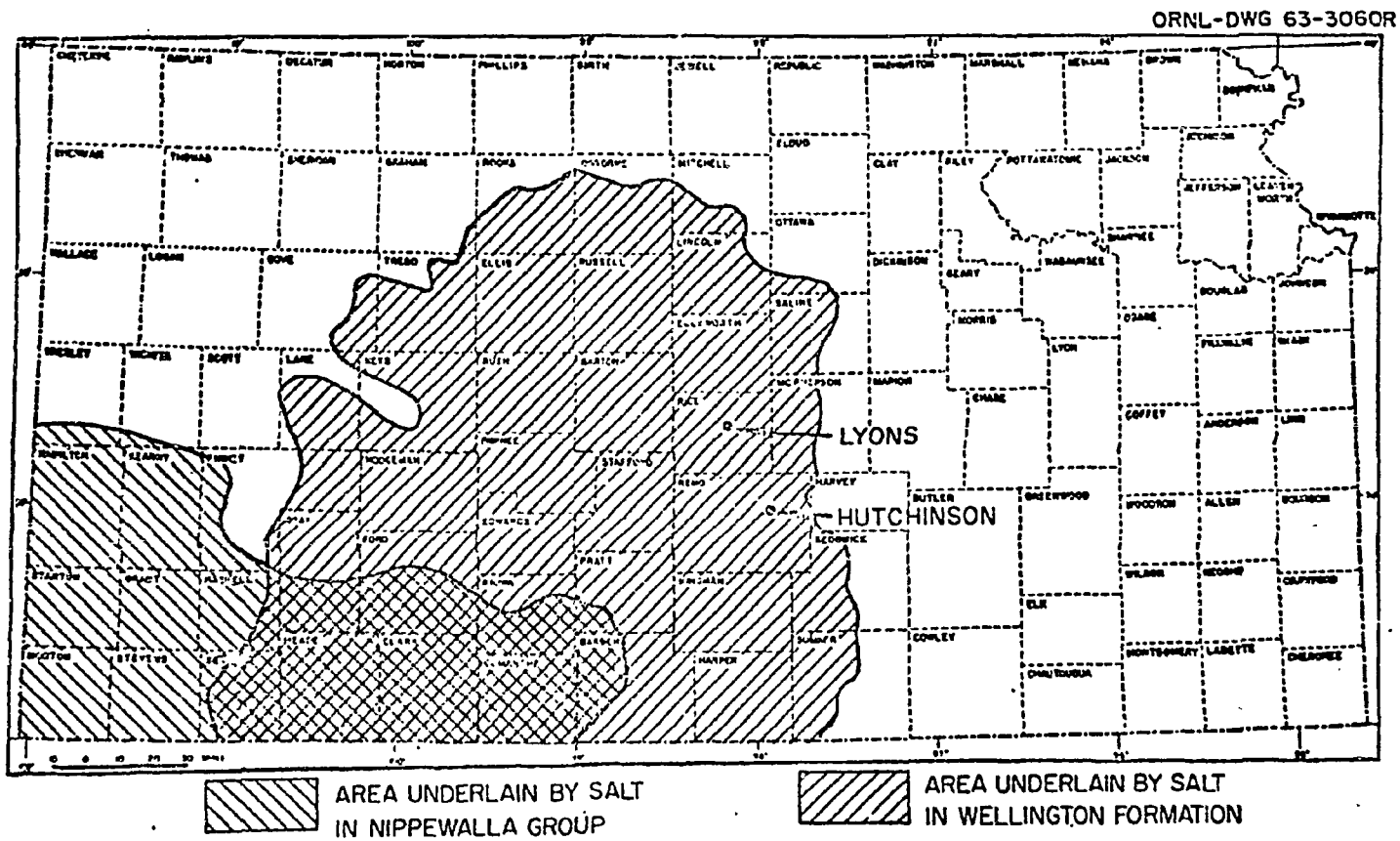

Figure 3. Location of salt-bearing formations in Kansas (from Bradshaw and McClain, 1971, p. 49).

CHAPTER II

EXPERIMENTAL METHODS

Sample Collection

Eighty-three samples (coded by the core number and depth) from two 4 inch (10.2 cm) drill cores were provided by the U.S. Atomic Energy Commission (now part of the Energy Research and Development Agency, ERDA). The samples, wrapped in plastic, were received late in 1974. One-half of each core was sent by the U.S.G.S. to Dr. Richard Beane, Department of Geosciences, New Mexico Institute of Mining and Technology, Socorro, New Mexico, for determination of their chemical compositions, water loss by thermogravimetry and normative analysis. Samples were selected to give maximum coverage in three priority zones which ERDA had designated as the most likely depths for the radwaste repository. In the nonpriority zones, samples were provided at intervals of approximately 40 to 60 feet. An attempt was made to select samples which contain some clay or other hydrous minerals in otherwise halite-rich rock. AEC #7 was drilled in Lea County, New Mexico 2040' (621.8 m) from the north line and 2040' (621.8 m) from the east line in Section 31 of Township 21-S and 32-E of the U.S.G.S. Hat Mesa quadrangle map. AEC #8 was drilled in Eddy County, New Mexico, 937' (285.6 m) from the north line and 1980' (603.5 m) from the west line in Section 11 of Township 22-S and Range 31-E of the Nash Draw quadrangle.

Sample Preparation

Since several methods of analysis (including X-ray diffraction and spectroscopy, petrographic analysis and water loss determinations) were to be performed the samples received had to be split into several parts. Due to the destructive nature of the sample preparation, the following procedures were used in making the samples for testing.

Samples to be thin-sectioned were prepared by cutting an approximate 8 cm × 4 cm × 1 cm slice from a representative segment of each core using a power saw with a dry, masonry-asbestos blade. The resulting slices were sent to Fred Roberts (Petrographic Section Service) of Monterey Park, California, who prepared the 4.8 × 7.2 cm (2 × 3 in) thin sections. The thin sections were cut and ground without using any water and the epoxy cement was not heated (to avoid causing any mineralogical changes in any hydrous minerals which might be present). Because of the cleavable nature of salt, some difficulty was encountered in the preliminary cutting of the slices which sometimes shattered. However, a large enough slab of each core segment was obtained to make an adequate 2" × 3" thin section.

A portion of each core adjacent to that cut for thin-sectioning was preserved intact for macroscopic observation and for making an additional thin section if needed. The remaining material from each core segment was passed through a rock crusher (which was cleaned after each core segment) and broken into 5 to 10 mm fragments which were split until a representative portion of sufficient quantity remained to prepare for analysis. One part of each portion was further crushed

using a porcelain mortar and pestle until approximately 5 grams could be sieved through the #60 but not #120 size mesh. The #60 to #120 size mesh material was bottled and used in the dehydration studies. The rest of the portion was again divided several times using a micro-splitter and the final split (about 10 grams) was completely crushed to pass a #325 size sieve. Pressed pellets were made by filling an aluminum cup (3 cm in diameter and 8 mm deep) approximately two-thirds full and placing the cup and its contents under 5000 psi pressure for 5 minutes. Pressed pellets were previously found to provide more uniform results and reproduceable patterns than hand packed mounts (Hidalgo and Renton, 1970). The pressed pellets could be stored and the same surface X-rayed again.

X-Ray Methods

X-ray diffraction analyses were performed by using a Norelco X-ray Diffractometer. The operating conditions are described in Appendix B. Preliminary mineral identification was facilitated by using a mylar overlay with the prominent peaks for halite, polyhalite, anhydrite and gypsum marked at the 2θ positions given by the Joint Committee on Powder Diffraction Standards. Many patterns were double-checked by overlaying known patterns with a sample pattern on a light table.

X-ray spectroscopy (fluorescence) was used to determine the bromine content of each sample. To avoid significant contamination by any sulfate minerals (which may alter the bromine content) new pressed pellets were made for each sample. Clear, cubic halite crystals with

a minimum of visible inclusions of any other material were crushed and sieved to pass a #60 size mesh. The crushed salt was quartered and a representative sample was made into a pressed pellet using the same techniques as with the samples prepared for X-ray diffraction.

Preliminary analyses were made using a Norelco Universal Vacuum X-ray Spectrograph to determine the relative purity of the samples and to determine the relative bromine content of the samples in order that three could be chosen to be used as standards in later, more precise analyses. In order to determine the purity of the samples, reagent-grade sodium chloride (which contained a reported 0.0005 percent (5 ppm) sulfate determined by wet chemical analysis). This is equivalent to about 3 ppm sulfur by molecular weight which the spectrograph would detect. The samples were run for sulfur on the Norelco Vacuum X-ray Spectrograph under the following conditions:

Source:	Tungsten anode	Crystal:	PET
Kilovolts:	35	Sample chamber:	vacuum .10 microns
Milliamps:	25	Energy detected:	S Kα1
Detector:	flow porportional	Recorder	
Kilovolts:	1.618	Time constant:	1 second
Gas:	P-10	PHA	
Flow:	0.25 scfm	Baseline:	200
Position:	75.85°2θ	Window:	350

Approximately one out of every three samples were checked for sulfur and the comparison between the standard (approximately 50 cps) and the samples (all less than 150 cps) showed no large amount of sulfur which might bias the results.

Based on the relative bromine contents, three samples were selected with "high" (137 cps), "medium" (87 cps) and "low" (31 cps)

bromine values and sent to the Oak Ridge National Laboratory, Oak Ridge, Tennessee for precise determination of their bromine contents. These samples were used as standards in the final analyses. Mr. J. Carter of the Analytical Chemistry Division performed the analyses using an isotope-dilution, mass spectrometry technique. The values obtained are shown in Table III.

TABLE III

ISOTOPE-DILUTION MASS SPECTROMETRY ANALYSES FOR SELECTING STANDARDS

Relative Bromine Contents	Duplicate Run Values-ppm	Estimated Content ppm ± 20%
"low"	18, 21	20
"medium"	25, 33	30
"high"	40, 60	50

The final bromine analyses, reported and discussed in Chapter IV, were performed using an ORTEC 6110 TEFA (tube-excited fluorescence analyzer) Spectrograph. A description of the instrument and the analytical procedure is given in Appendix A.

Dehydration Studies

Dehydration studies were performed on representative samples from each core sample by Dr. O. C. Kopp, Department of Geological Sciences, University of Tennessee, Knoxville, to determine the water losses of these samples when subjected to heat (as might occur when radioactive

waste canisters are buried in saltbeds). Samples of the #60-120 size material (approximately 1.5 to 2 grams) were weighed, heated at temperatures ranging from 100° to 300°C for periods from 2 days to 6 weeks and weighed again to determine the amount of water lost. The procedures used were essentially the same as for the dehydration studies conducted on the Hutchinson Salt Member of the Wellington Formation near Lyons, Kansas (Kopp and Fallis, 1973). Details of the water-loss analyses for the Salado Salt were presented in the Final Report for this study (Kopp and Combs, 1975).

CHAPTER III

MINERALOGY AND PETROLOGY

Introduction

The lithology of drill cores AEC #7 and #8 is shown in Figure 4. The major minerals present in the samples taken for this study from the cores include halite, anhydrite, polyhalite and clays and silt-sized minerals (quartz, feldspars and magnesite). In addition, several minor and/or trace minerals such as sylvite, carnallite, celestite, glauconite and possibly kainite were detected. Schaller and Henderson (1932) in an earlier study of 41 private and government cores from the potash district of New Mexico and west Texas also observed a large number of rare evaporite minerals including bloedite, carnallite, epsomite, glauberite, kainite, kieserite, langbeinite, leonite and lueneburgite. Perhaps the reason why many of the less common minerals were not observed in this study is that the samples were chosen from the cores "to avoid obvious nonsalt (potash) formations" (McClain, Lomenick and Lowrie, 1975, p. 7). Anhydrite was second in abundance below 2427' (739.7 m) in AEC #8 and 2702' (823.6 m) in AEC #7 and made up a large portion of the sections above these depths. Polyhalite is very common and next in abundance after halite and anhydrite. Clays, quartz, feldspars and what was probably magnesite were often seen together. Sylvite was observed in a few thin sections but made up a small part of the total mineralogy. The remaining trace minerals were in such

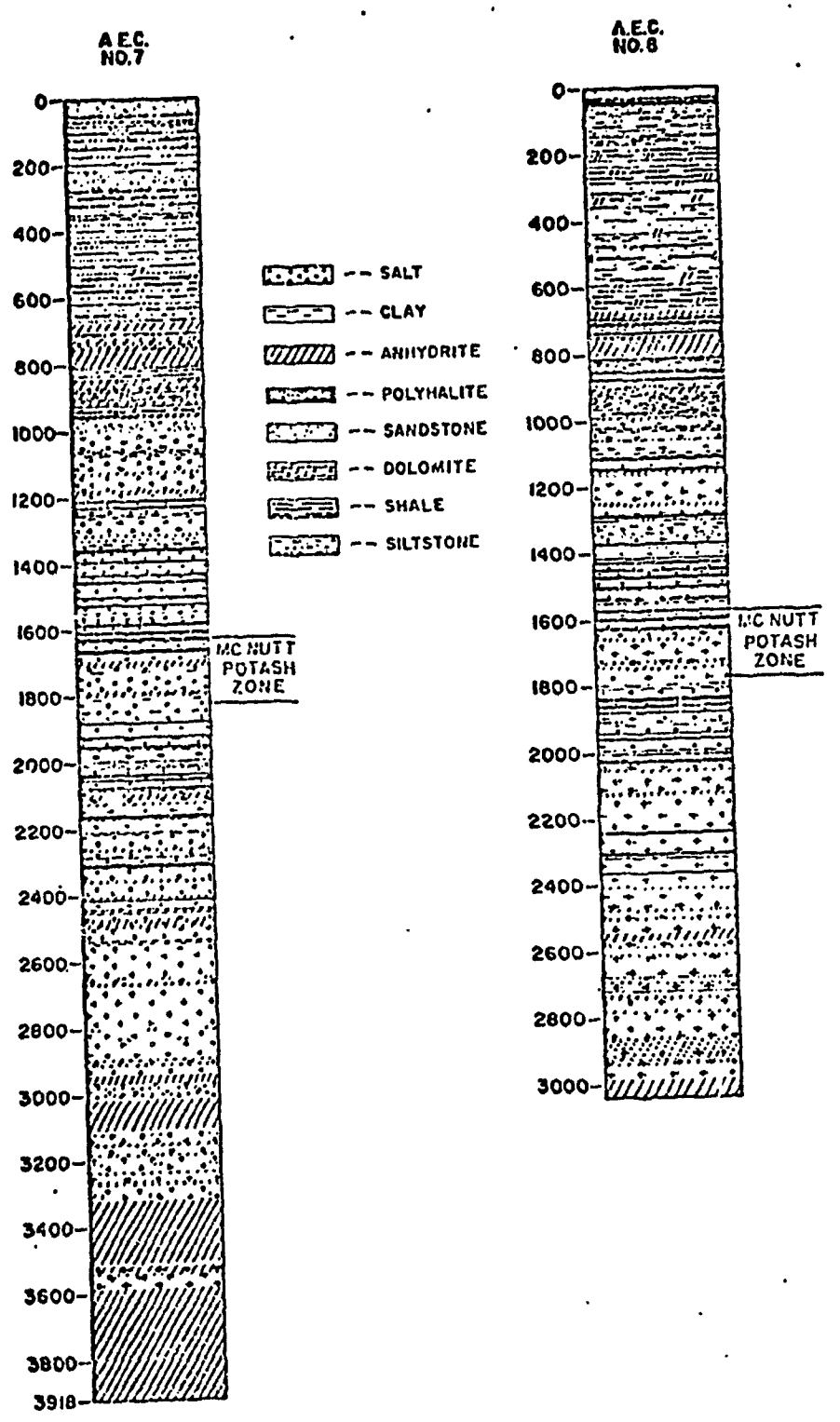

Figure 4. Lithologic columns for cores AEC #7 and #8. Thickness of polyhalite beds is slightly exaggerated.

limited amounts and/or small grain size that positive identification was not always possible. The mineralogy of both core samples by X-ray diffraction analysis is given in Appendix B and the descriptions of the thin sections are given in Appendix C.

Mineralogy and Petrology of the Salado Salt

Halite. Halite (NaCl) constitutes the major mineral in most of the thin sections. Generally, halite appears in the form of colorless crystals ranging in size from less than 1 mm to well over 3 cm with distinct grain boundaries. Halite crystals possess numerous to rare inclusions (depending upon the individual crystal) which often take the shape of negative cubic cavities, some of which contain solid, liquid and/or vapor phases. Other cavities contain dark, petroliferous material.

The spatial arrangement of the inclusions is interesting. While most are scattered more or less randomly through the halite, many inclusions are often aligned along grain boundaries and distinctly outline individual crystals. Still other inclusions are aligned parallel to cube faces and intersect at right angles (Plate 1). (All plates are in Appendix D.) Such features are called "hopper crystals" which are formed when cubic halite crystals precipitate from sodium chloride saturated seawater (Figure 5, #1) and slowly sink since they are of higher density than the brine. As the crystals sink beneath the surface, growth occurs along the lateral sides of the cubes which are held at the water-air interace by surface tension (Figure 5, #2 and #3). As growth and sinking of the crystal continue, an inverted pyramid with a hollow center develops

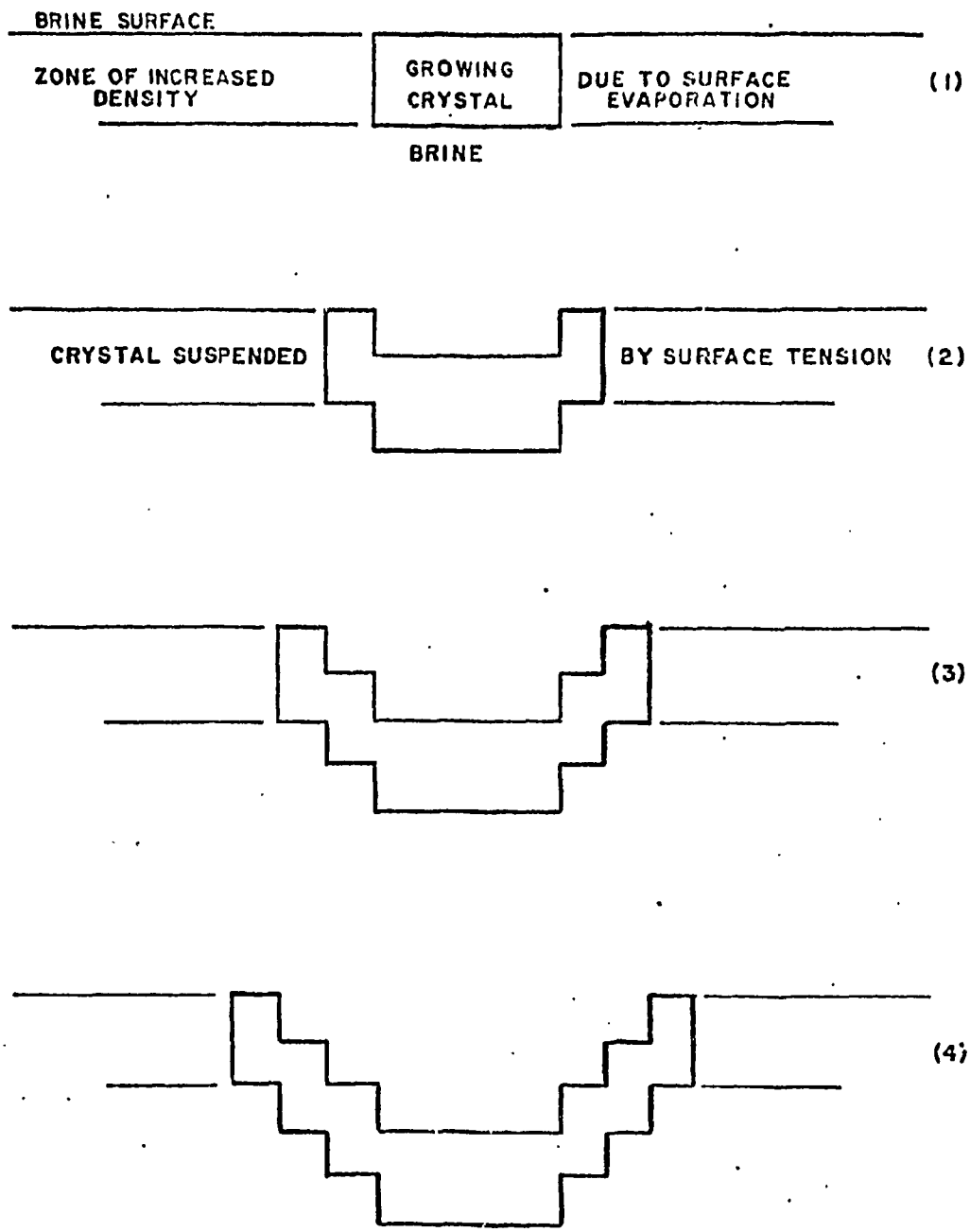

Figure 5. Development of a Hopper Crystal (after Dellwig, 1955, p. 89).

and finally drops to the bottom (Figure 5, #4). The presence of hoppers is thought to indicate quiet and presumably relatively shallow water since the process of hopper crystal formation and preservation is so delicate. It would seem unlikely that numerous well preserved hoppers would be deposited in a deep water basin. Depths of several hundred feet or less are thought by this author to be more conducive to the preservation of hopper crystals. In the thin sections of the Salado Salt, hopper crystals are observed in about half of the samples.

Fracturing, from minor to severe, is evident in most of the halite-bearing slides from the Salado. Several factors may be responsible for such features. In situ deformation resulting from regional or local deformation may be one cause of fractures. However, post-Permian tectonics are thought to be mild in this region (Claiborne and Gero, 1974, p. 41) and would not account for the intense fracturing exhibited in some of the thin sections. A more logical explanation for many of the fractures would involve expansion of halite upon the release of confining pressures when cored and brought to the surface. Also, the preparation of the thin sections undoubtedly caused some of the fractures since they are especially evident at the edges of the thin sections. However, some fractures must have been present prior to coring because they contain trapped liquid and/or solid phases.

The halite in the Salado thin sections is made up of subhedral to nearly euhedral crystals usually with distinct grain boundaries marked off by inclusions and/or petroliferous seams. Between crossed-nicols halite is isotropic which allows excellent viewing of the anisotropic

minerals present. When initially deposited, the halite was probably very porous and permeable allowing later solutions to move freely between the crystals. However, as more overburden pressure was applied the halite was compressed into a more solid mass, new minerals could form only along grain boundaries. Patches (regular to irregular, equidimensional areas) and stringers (usually irregular, elongated areas) of clay and silt-sized material were also often trapped between the grains (Plate 2). Even in the compacted state solutions were not totally restricted from passing through the halite (especially along grain boundaries and fractures) and altering the primary minerals. Clay patches seem to have been areas of such activity because of the association between clays and several minerals. Coarse, isolated crystals of anhydrite and/or polyhalite appear within halite crystals or appear to be growing from the grain boundaries into halite crystals. These minerals probably formed rather late and replaced part of the halite.

Anhydrite. Anhydrite ($CaSO_4$) is the major sulfate mineral in the cores and comprises an appreciable amount of the core in the lower part of the section studied. It is a biaxial mineral which exhibits various habits. It occurs in fibrous, prismatic and tabular crystals and is often twinned or lamellar. Optically, it is distinguished from polyhalite by several properties as shown in Table IV.

TABLE IV

PROPERTIES OF ANHYDRITE AND POLYHALITE

Properties	Anhydrite	Polyhalite
crystal system	orthorhombic	triclinic
relief	(+) mod., varies	(+) low
birefrigence colors	3° green	2° blue
sign	(+)	(-)
extinction	parallel, symmetrical	oblique
cleavage	often right angles	---

Anhydrite is chemically equivalent to gypsum (minus water) and often occurs as a secondary mineral after gypsum. It is also deposited as a primary mineral by the evaporation of seawater at temperatures above 42°C or at lower temperatures with increased salinity (Mason and Berry, 1968, p. 364).

Anhydrite appears in several habits and associations. A fine-grained, fibrous variety occurs in large patches similar to polyhalite. Distinguishing between the two in this habit is very difficult. These patches of anhydrite are not associated with fractures, clay patches or grain boundaries and probably can be considered as primary anhydrite. This fine-grained anhydrite often occurs in nodular masses and is thought to have been deposited in shallow water. This is more apparent in the samples from greater depths, typically below 2500 feet (762 m). Another form, subhedral to euhedral anhydrite in prismatic or acicular crystals (sometimes twinned) can be observed along fractures, in grain boundaries and within halite crystals. These crystals sometimes occur in a

spherulitic shape (starburst). The origin of these crystals is not certain. Those in fractures or in grain boundaries might be secondary but similar crystals occur within large halite grains indicating a replacement origin. Anhydrite also occurs in large, cross-twinned crystals as distinct pseudomorphs after "swallow-tail" gypsum. These are definitely of secondary origin.

Replacement of anhydrite by polyhalite is common. This alteration and association will be discussed under the section on polyhalite. Bedded anhydrite occurs and can be recognized even in thin sections [AEC #8: 1652' (503.5 m), and 2563' (781.2 m)].

Polyhalite. Polyhalite [$K_2MgCa_2(SO_4)_4 \cdot 2H_2O$] is the most common potash mineral observed in the cores examined and occurs in several habits and associations. Optically, it is a biaxial mineral with generally low birefringence (1° pale yellow). Thicker sections may show some 2° blue.

According to Braitsch (1971), polyhalite can occur in habits from tabular to prismatic or fibrous, and is always twinned. In the Salado Salt it is typically very fine-grained, almost to the point where individual grains are microscopically indistinguishable. The fine-grained, massive variety is usually found in patches, between grain boundaries, filling fractures (Plate 2) in the shape of stringers and possibly deformed by flowage (Plate 3). In some thin sections [such as AEC #8: 1652' (503.5 m)] massive, fine-grained polyhalite is the dominant mineral. Isolated polyhalite crystals (or small clusters of crystals) often have acicular to prismatic habits. These crystals

(and crystal clusters) often form starbursts with seed crystals (Plate 4). The isolated crystals appear to be authigenic.

Polyhalite is intimately associated with halite, anhydrite and clay and silt-sized minerals. It is often disseminated throughout halite, appearing as reddish-orange blebs or tinting large areas of halite with a red to orange color. The color associated with polyhalite (and some other potash minerals) stems from the presence of finely-disseminated iron oxide (Schaller and Henderson, 1932, p. 37).

Polyhalite also appears to be bedded in some thin sections [such as AEC #8: 1652' (503.5 m), 1986' (605.3 m), 2366' (721.2 m)] usually associated with anhydrite and apparently is secondary. Many thin sections show fine-grained polyhalite adjacent to coarse crystals of anhydrite which have serrated edges due to replacement by the polyhalite (Plate 5). Further away from such replaced areas polyhalite is often present in coarser crystals. These features clearly indicate secondary replacement of anhydrite by polyhalite.

Clay and silt-sized minerals. Clay and silt-sized minerals include clays, quartz, feldspars in varying quantities and are often associated with polyhalite and anhydrite. This relationship may be due to two factors. First, the areas which contain the clastics are relatively porous regions which may have allowed fluid movement around the relatively impermeable, compacted halite. Secondary alteration of primary minerals or deposition of new minerals from flowing, concentrated brines are likely in these places. Second, the phyllosilicate clay minerals can be

good sources of potassium and magnesium from which polyhalite might form if a calcium-rich brine were to come in contact with it. These clastic regions tend to form in patches and stringers along grain boundaries. Some thin sections also show subhedral to euhedral cubic halite crystals imbedded in clays and silt (Plate 6). This appears to be a feature of a semiexposed tidal flat which produced halite crystals that became covered with terrigenous matter. Clays are also disseminated through halite crystals in many cases (Plate 7) and must have been incorporated as the crystal grew. Some clay patches show obvious dessication and resulting cracks. Whether this is the typical "mud crack" is unknown (Plate 8).

Magnesite. While magnesite ($MgCO_3$) was not positively identified in thin section, its presence was detected by X-ray diffraction in many samples and was very prominent in the X-ray pattern of one section [AEC #8: 2563' (781.2 m)]. It is a typical uniaxial rhombohedral carbonate with high birefringence (0.191-0.199) and has a pearly to high order white color. Several grains observed possibly fit the description but none were positively identified due to limited quantity and small grain size. Magnesite was usually associated with the clay and silt-sized constituents but has been observed by other workers to occur in thin bands of pure magnesite. No other carbonates (calcite and dolomite) were detected in this study or that by Schaller and Henderson (1932).

Sylvite. Sylvite (KCl) was observed in several thin sections in the vicinity of polyhalite. Being isotropic like halite, the presence of the mineral was confirmed by its purplish-red color due to iron

oxide inclusions and a higher (but negative) relief than halite (Plate 7). It was observed in this study as small isolated grains with no discernible crystal form. Like halite, sylvite has perfect cubic cleavage (Braitsch, 1971). In the potash zones, sylvite is often intermixed with halite and this mixture is called sylvinite. Sylvite occurs in a red-colored variety and in a milky white-colored variety apparently representing a different paragenesis (Borchert and Muir, 1964, p. 220). It is one of the more economically-valuable potash minerals because of its high potassium content (63.2 percent K_2O), but unfortunately precipitates only under conditions of extreme concentration because of its high solubility. It is not likely that sylvite was deposited in large quantities during most of Salado time except for a short span when the McNutt Potash zone resulted.

Carnallite. Carnallite ($K_2MgCl_3 \cdot 6H_2O$) was detected in one thin section adjacent to a carnallite zone as indicated by the well log. It occurs in a variety of colors from clear to white to red and sometimes has a metallic luster. Carnallite takes several habits such as thick tabular, pyramidal, granular and fibrous with no cleavage but with a conchoidal fracture. Its birefringence is relatively higher than other evaporite minerals (0.028). Schaller and Henderson (1932) noted an occurrence of carnallite as blebs and streaks in anhydrite and associated polyhalite suggesting a possible replacement phenomena.

Celestite. Celestite ($SrSO_4$) was tentatively identified in several thin sections based on its relatively high relief and spear-shaped,

elongated crystals. It was very similar to some forms of anhydrite except for the terminus of the crystal.

Kainite. Kainite [$K_4Mg_4Cl_4(SO_4)_4 \cdot 11H_2O$] was probably observed in one thin section. It is a monoclinic mineral with moderate birefringence (0.022) and occurs in thick tabular, massive and fibrous habits with a variety of colors.

Glauconite. Glauconite [$K(Fe,Mg,Al)_2(Si_4O_{10})(OH)_2$] was observed as round, greenish grains in a few places. As reported by Mason and Berry (1968, p. 454) it is a mica which is presently forming on the sea floor where clastics sediments are few or lacking. Conditions in evaporite basins would be analogous to those on the sea floor except for the differences resulting from the shallow depth of water.

Mineralogy and Petrology of the Hutchinson Salt

The mineralogy and petrology of the Hutchinson Salt (as taken from the thin sections of the previous study by Kopp and Fallis, 1973) varies from that of the Salado Salt. The mineralogy is different for that of the Salado since the Hutchinson Salt contains gypsum in large quantities, dolomite and larger amounts of clays. The gypsum is present primarily at more shallow depths [above 620 feet (188.9 m)]. This is to be expected if it was not buried at sufficient depth to be dehydrated to form anhydrite.

The most noticeable petrographic difference is the macroscopic bedding of many thin sections of the Hutchinson Salt. Most of the bedding is due to laminated shales, claystones and siltstones. Not only

was cross-bedding observed but so was rhythmic graded-bedding in many thin sections. Graded bedding appears first as a sharp basal contact, progressing from coarser grains near the bottom into fine grains at the top. This is eventually terminated by another sharp contact and repeated again.

Halite is the dominant mineral in the middle depths of the cores and contained many of the same features and associations as the halite in the Salado. Fractures are common, as was petroliferous material. Anhydrite and polyhalite are dispersed throughout the halite, filling fractures, in patches and stringers and forming starbursts. Anhydrite is more abundant in the deeper core sections and was the dominant material in some of these sections.

The Hutchinson appears to have been closer than the Salado to a source of terrigenous material and hence received a greater amount. It also appears to have been formed in a less arid environment or formed from a less concentrated brine based on the lack of exotic minerals in any part of the Wellington.

The petrography of the Wellington is discussed in more detail by C. L. Jones (1964).

CHAPTER IV

BROMINE GEOCHEMISTRY OF MARINE EVAPORITES

Introduction

Marine evaporites develop by the concentration (by evaporation) of undersaturated solutions provided by seawater influx, stream drainage and rainfall. Logically, evaporite minerals are composed primarily of constituents in seawater. It is generally believed that the composition of the ocean has not changed significantly since Paleozoic time (Borchert and Muir, 1964, p. 18) and hence, assumptions can be made as to the origin of ancient evaporite deposits by studying the makeup of present day-oceans. One of the most frequently studied elements in evaporite minerals is bromine. Boeke (1908) first investigated the substitution of bromine for chlorine in potassium, sodium, and magnesium chloride minerals.

Bromine in Evaporite Deposits

Seawater contains on the average 65 ppm bromine and 18,980 ppm chlorine with a ratio of 292 Cl^-/Br^- (see Table I, page 5). When evaporation of seawater in a restricted basin occurs, chlorine is incorporated into the formation of halite (NaCl), sylvite (KCl), and carnallite ($K_2MgCl_3 \cdot 6H_2O$). Bromine, however, is a dispersed element. As chlorine becomes saturated to its maximum point and salt precipitation occurs (which maintains the chlorine balance), and bromine becomes more and more concentrated since it does not precipitate and form its

own mineral species. Bromine substitutes only partially for chlorine, but as its concentration increases so does the amount of substitution between chlorine and bromine. At temperatures of formation of evaporites, bromine is completely diodochic with chlorine and forms a continuous solid solution series from KCl to KBr. Bromine will not, however, substitute completely for chlorine through the series NaCl to NaBr; hence, sylvite (KCl) contains more bromine than halite (NaCl) (Adams, 1967, p. 44). The reason for this preferential adsorption is that Br^- (1.95 Å) tends to form an ionic bond with a cation close to its own size and K^+ (1.33 Å) fits better than Na^+ (0.95 Å). This may be why bioschofite ($MgCl_2 \cdot 6H_2O$) (Mg^{++}=0.65 Å) does not incorporate relatively large amounts of bromine.

The partitioning of bromine between the brine and the solid is unique for each mineral. Kühn (1955) defined this partitioning in terms of a bromine distribution coefficient (b) which is shown as:

$$b = \frac{\text{wt. \% Br crystal}}{\text{wt. \% Br solution}}$$

Braitsch and Herrman (1963) showed the coefficient as being approximately 0.15 for halite, 0.52 for carnallite and 0.81 for sylvite at 25°C in a $MgCl_2$-free solution with the bromine concentration below 1 percent. The coefficients do not hold true when the bromine concentration is higher than 1 percent but this does not occur in evaporite brines. Magnesium chloride solutions do noticeably decrease b and must be taken into consideration when interpreting the relationships. The ideal concentration at which halite first crystallizes is 0.0075 percent Br/NaCl (75 ppm). In static evaporation the bromine content should increase

logarithmically until potash minerals are deposited at 200-250 ppm. This smooth logarithmic increase is not the case in natural salt deposits and most show an erratic bromine profile (one which shows no rhythmic increase or decrease but irregular fluctuations). Periodic influxes of seawater lower the total bromine concentration in the basin and therefore decrease the amount of bromine incorporated in each mineral species. Dilute brine influxes should not produce such erratic patterns in deep water models since mixing of incoming low density brines with concentrated high density brines would not be as complete as in shallow water basins. Instead, influxing seawater would flow on top, as precipitation of evaporite minerals continues from the bottom-lying, unaltered brines.

Adams (1967, p. 49) stated five conclusions which can be reached on the basis of bromine profiles of salt deposits:

1. the degree to which brine evaporation has occurred should be indicated by higher bromine content,
2. bromine profiles can be used as prospecting tools for locating the stratigraphic proximity of potassium minerals,
3. vertical and horizontal changes in bromine content should provide information on variations in brine composition with time and position in the basin,
4. secondary halite deposited from a preexisting deposit can be distinguished from primary halite by its lower bromine content,
5. bromine profiles for an evaporite should supplement lithology as a means of lateral correlation.

Bromine in the Salado Salt

Bromine in the Salado Salt has been studied by previous workers with approximately the same results as those derived in this study. Holser (1966) presented an erratic profile of bromine content from depths of 400 feet (121.9 m) (in the Salado) to 4100 feet (1249.7 m) (in the Castile) (Figure 6). He recorded values ranging from 20 ppm bromine at the base of the Salado to values from about 20 to less than 90 ppm throughout the upper portion of the formation. Adams (1967) made a comprehensive study of the bromine distribution in the Salado Salt and, likewise, showed an erratic profile with most values between 40 and 80 ppm bromine from a core depth of 400 feet (121.9 m) to 860 feet (262.1 m) (Figure 7).

The bromine analyses done in this study were made before the author became aware of the work done by S. A. Adams (in fact, a copy of his unpublished dissertation was not received until the initial writing stage of this thesis). The results of this study generally support the data presented by Adams (and Holser). Correlating with the base of the Salado and the 10th potash ore zone, this study covers about the same stratigraphic horizons as Holser's profile. It is not known what exact stratigraphic horizons are covered by Adams' sample interval, but it is assumed to be roughly equivalent to that covered by Holser and this study. Forty-eight samples between 1400 (426.7 m) and 2950 feet (899.2 m) in AEC #8 and twenty-five samples between 1045 (318.6 m) and 2735 feet (833.6 m) in AEC #7 were analyzed. Profiles for both drill cores (Figure 8) show little in the way of a predictable profile as suggested by theoretical data. In fact, none of the samples analyzed showed

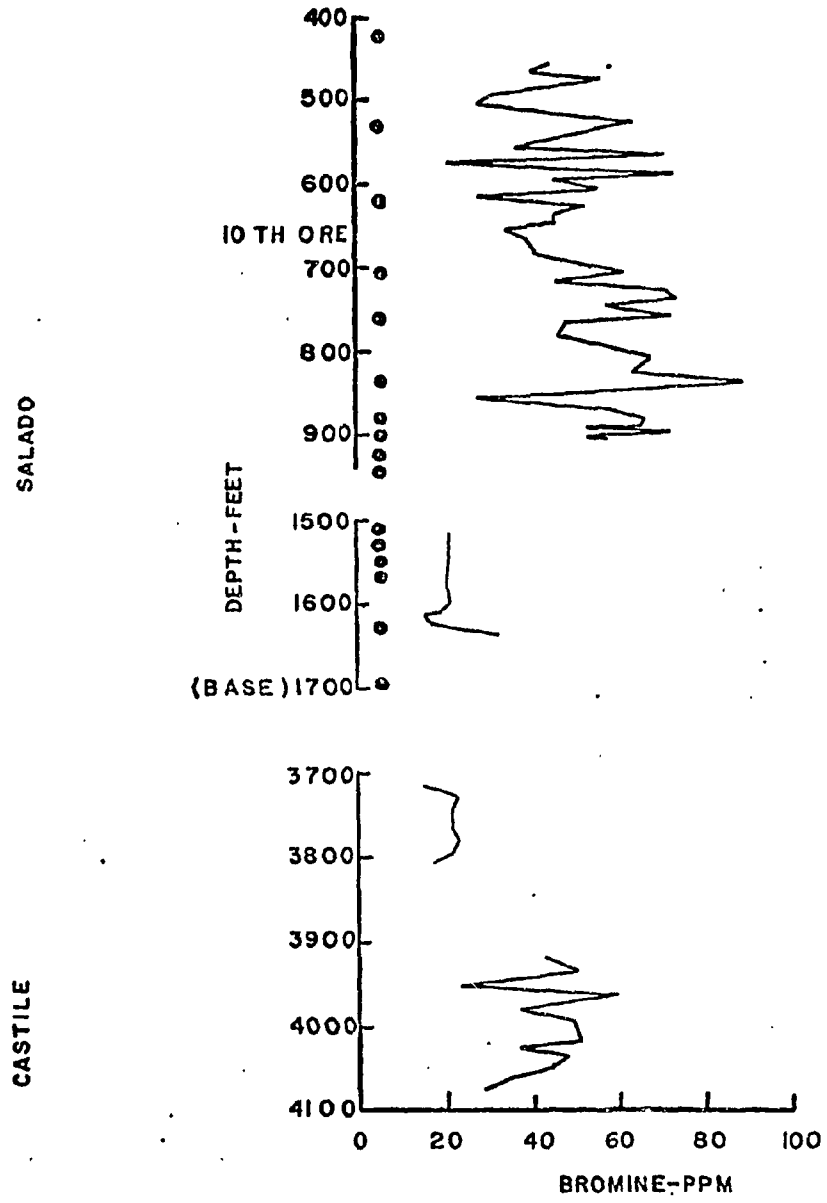

Figure 6. Bromine profile of the Salado Salt after Holser (1966, p. 263).

Dots along the ordinate are approximately equal to stratigraphic levels sampled in the Salado core AEC #8.

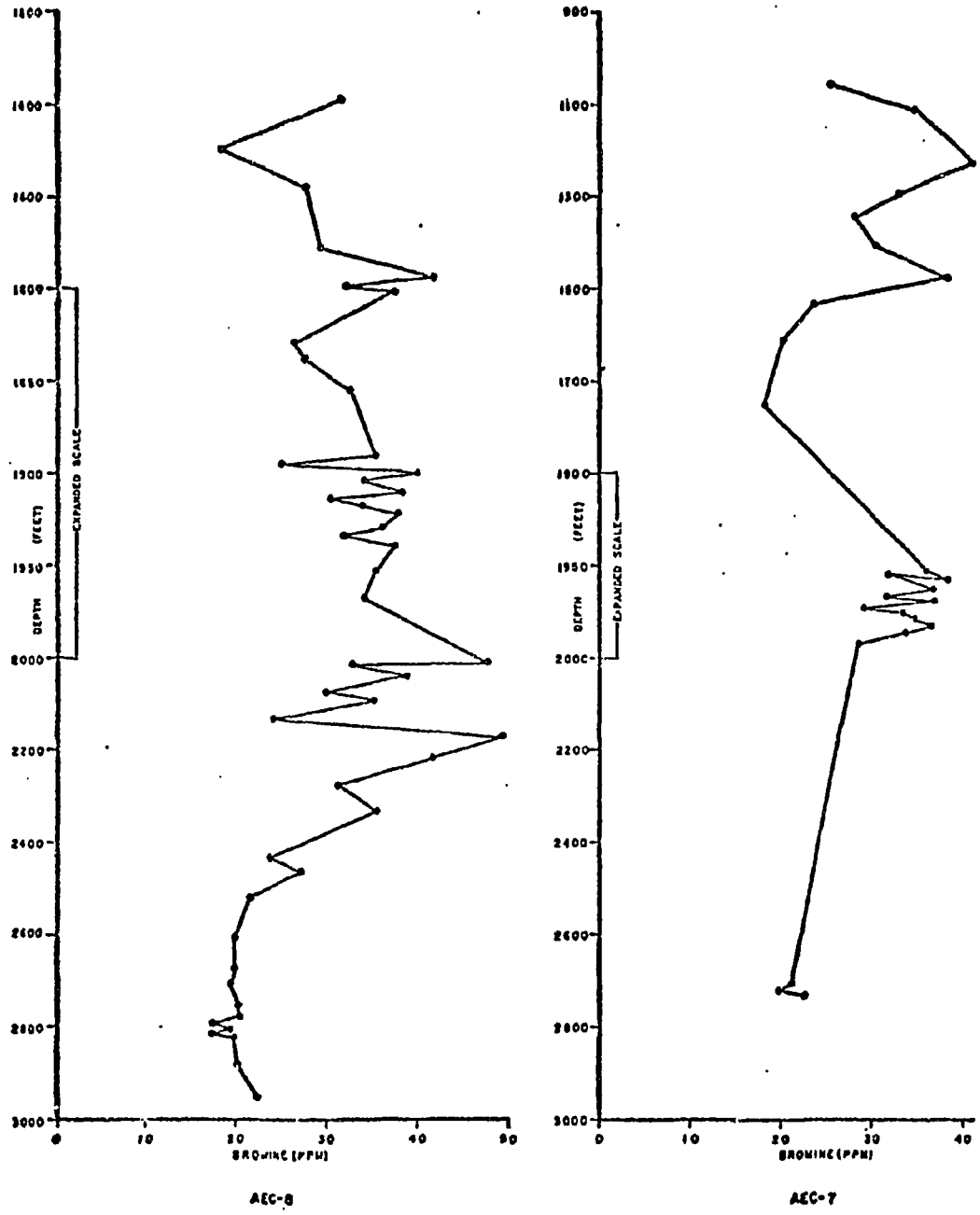

Figure 8. Plot of bromine content versus depth for cores AEC #7 and #8.

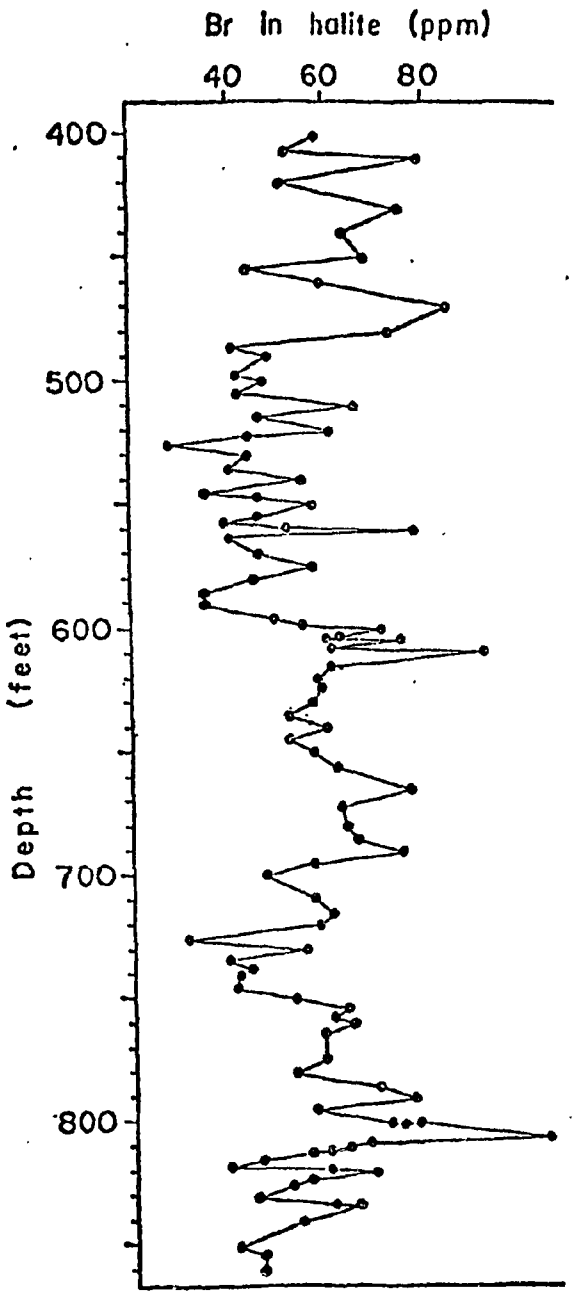

Figure 7. Bromine profile of the Salado Salt after Adams (1967, Figure 15).

bromine concentrations equal to or above that which should be incorporated into halite as it first crystallizes from normal seawater. The basal portion of the interval covered by AEC #7 and #8 agrees with Holser's values (approximately 20 ppm). The upper part of the interval fairly well agrees with the base of the profile by Adams (20 to 40 ppm) if it can be assumed that it represents the same stratigraphic horizon as in this study.

On the other hand, the results of this study do not support Adams' statement (1967, p. 78) that there exists antipathy between sulfate minerals (including disseminated and blebs of polyhalite) and high bromine content. While it is true that bromine is generally low when associated with anhydrite alone (below 2500' (762 m) in AEC #8), plots of relative polyhalite content (based on X-ray diffraction intensity of the major polyhalite peak at 2.92 dÅ) versus bromine content generally show a positive correlation (Figure 9). This relationship was not expected because polyhalite contains no bromine itself and therefore acts only to dilute the total concentration of bromine in a sample if it is present. Dilution by polyhalite should only become a factor if it was present in a sample which was thought to be pure halite. Samples from both cores were randomly checked for sulfur contamination (see Chapter II, p. 17) which would indicate the presence of sulfates such as polyhalite.

The relationship between increasing polyhalite content and higher bromine concentration is a curious one. It might be expected if the polyhalite were primary, but even then the bromine values of

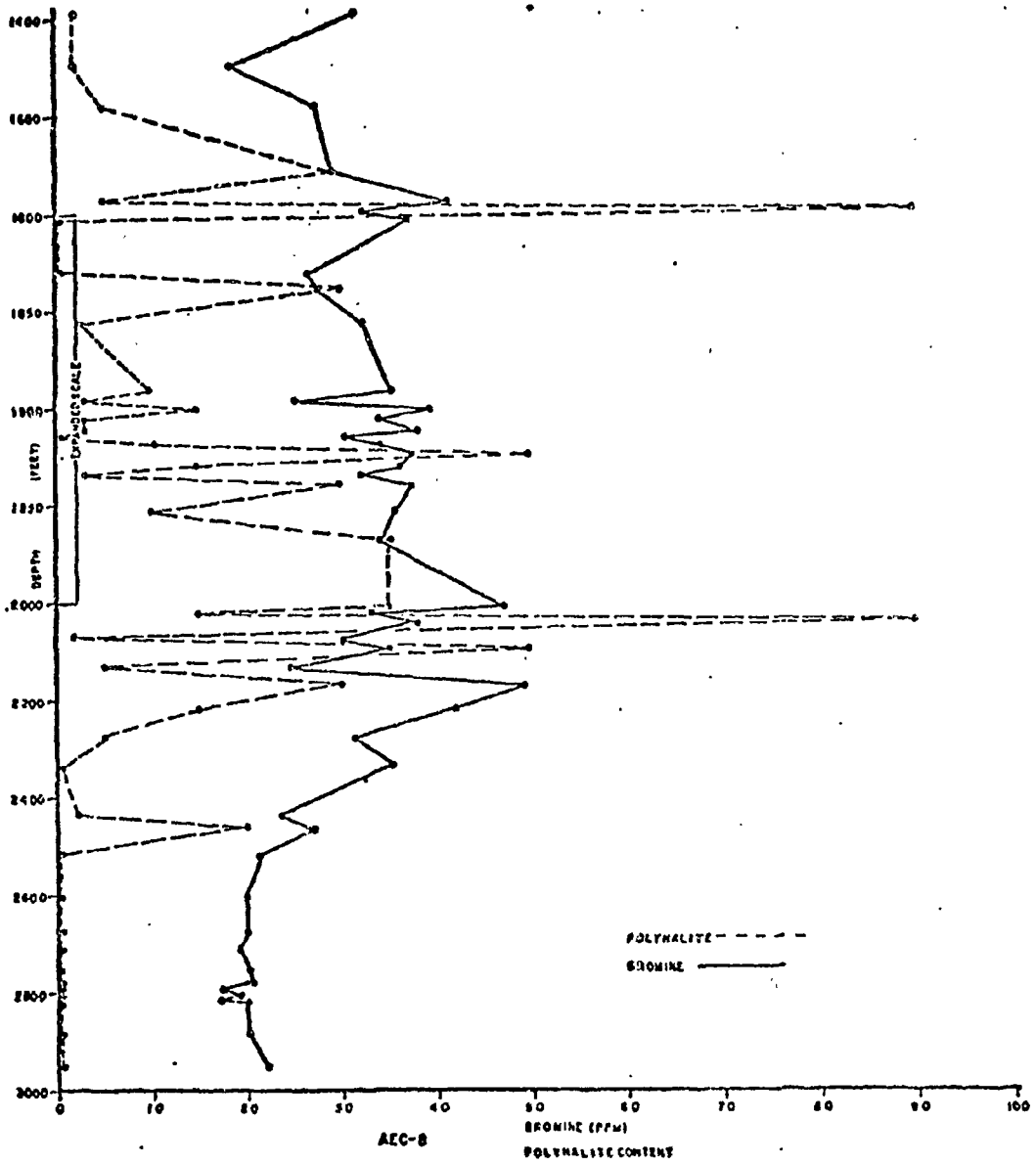

Figure 9. Profile of bromine content compared with relative polyhalite content.

Polyhalite content based on relative intensities of major peak at 2.92 Å

the associated halite should be four to five times what they are. It is unfortunate that in three samples [AEC #8: 1652' (503.6 m) 1986' (605.3 m) 2366' (721.1 m)] in which polyhalite was the dominant mineral (or codominant with anhydrite) halite could not be separated from the crushed core material and analyzed for bromine. These sections might be possible zones of primary polyhalite deposition.

Regardless of whether the polyhalite is primary or secondary, the values of the highest bromine concentrations are still far below the theoretical amount incorporated in halite when it first crystallizes from normal seawater. Two possible conclusions can be drawn. First, the bromine profile of the Salado as determined in this study (as well as Holser's and Adams' studies) appear to be that of a secondarily-deposited evaporite sequence. A preexisting evaporite deposit with a "normal" bromine profile was dissolved (thereby reducing its bromine content), carried in solution to the present location and recrystallized to form the Salado Salt sequence. (This conclusion assumes that the Permian seas were like that of present-day seas.) Second, whatever the origin of the polyhalite, there seems to be a relationship between high(er) bromine contents and greater amounts of polyhalite being present. Whether this is due to some stratigraphic factor, alteration of halite by the polyhalite-depositing solutions or to the recrystallization of halite along with polyhalite is uncertain because of the widely spaced and limited number of samples examined. This relationship should be a point for a more thorough investigation.

While discussing polyhalite in the Salado Salt one other observation can be made concerning the relationship between polyhalite content and water loss upon heating. (The relationship between clay minerals, and water loss at 100°C is discussed in the Final Report for this subcontract by Kopp and Combs, 1975.) The water loss data at higher temperatures was provided by Beane and Popp (1975). The relative polyhalite content was based on X-ray diffraction intensities of the major peak (2.92 Å). It was discovered that by plotting these two curves together an extremely good correlation between the amount of water loss upon heating and the amount of polyhalite present could be achieved (Figure 10). Not only do peaks for both curves match but so do most of the troughs. Polyhalite with its 2 molecules of water can contribute up to 6 percent water at high temperatures. Undoubtedly, clays are a major source of water in the Salado Salt (gypsum is not present in any quantity) at lower temperatures but at higher temperatures (above 300°C) polyhalite may make a significant contribution.

In addition to the bromine analyses performed for the Salado Salt bromine concentrations were determined for samples from two drill cores (AEC #1 and #2) in the Hutchinson Salt near Lyons, Kansas. Because of the large amounts of clay and other minerals present, only 14 samples for AEC #1 and #2 could be prepared. With so few samples it would be of little advantage to show a bromine profile for the Hutchinson Salt. However, the values obtained were comparable to those of the Salado Salt. Within the interval 816 (248.7 m) to 1077

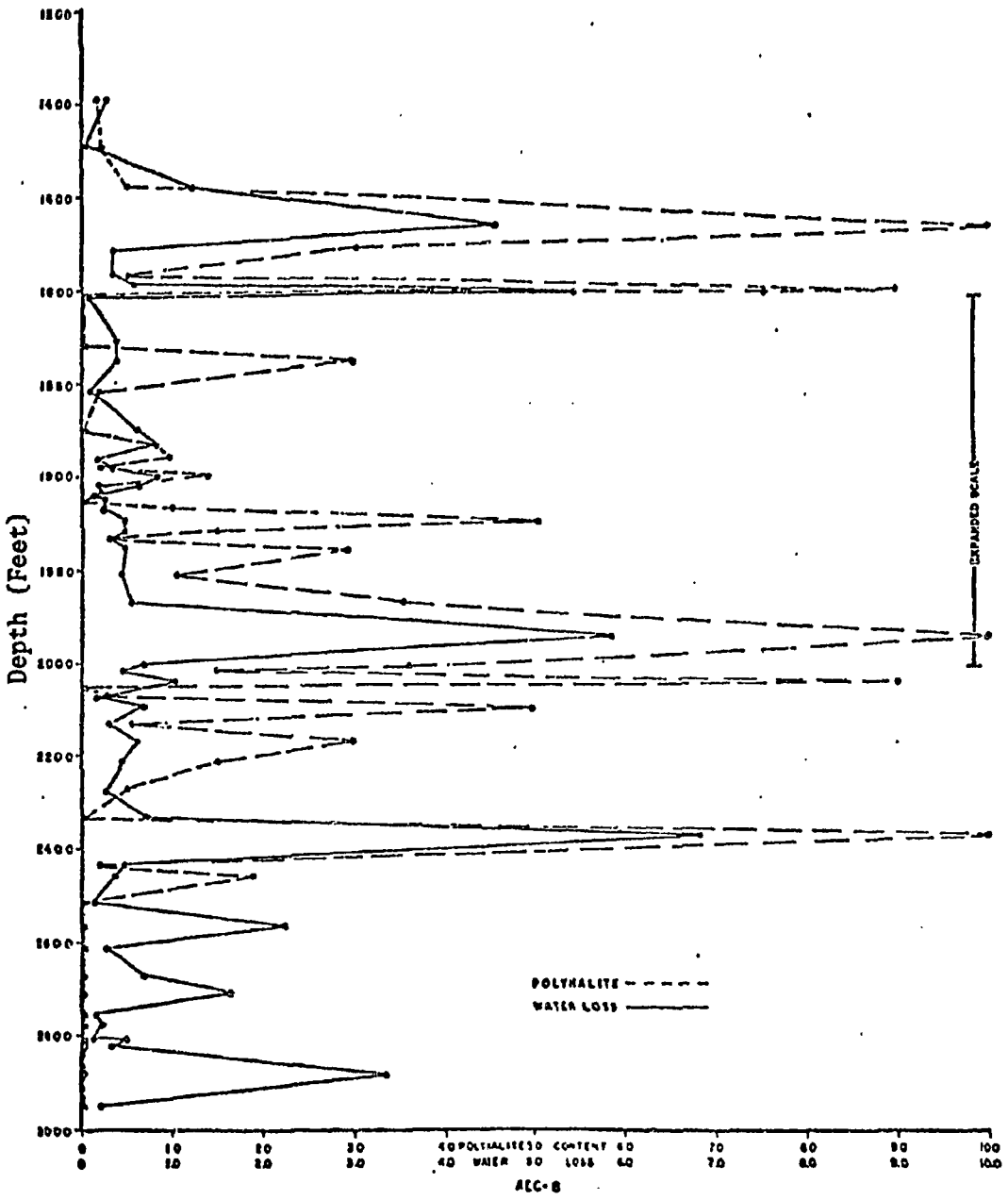

Figure 10. Profile of polyhalite content compared with total water loss (by weight percent) at 400° C.

Polyhalite content based on relative intensities of major peak at 2.92 Å.

(328.3 m) feet in AEC #1 and 790 (240.8 m) to 1002 feet (305.4 m) in AEC #2 all bromine values ranged from 21 to 42 ppm with most in the 30 to 40 ppm range. These results would seem to indicate that the Hutchinson Salt (part of the Wellington Formation) had the same type of genesis as the Salado. Holser also called the Wellington a "second cycle" salt (1966, p. 342).

CHAPTER V

SUMMARY AND CONCLUSIONS

The main purpose of this study was to determine the presence and quantity of water-bearing minerals in the Salado Salt near Carlsbad, New Mexico so that the formation could be considered for a potential radwaste repository. It was found that the Salado Salt dehydrates to a lesser degree than the Hutchinson Salt Member of the Wellington Formation near Lyons, Kansas, because of the general absence of gypsum and less abundance of clays. The Salado Salt loses up to a few tenths of a percent water in the purer halite beds. Where clays are abundant several percent of water (by weight) may be lost and in polyhalite zones as much as 5 or 6 percent water may be given off at temperatures near 300°C.

It is clear that the Salado Salt is a favorable site for radwaste disposal in terms of water loss. However, zones of clay and polyhalite must be avoided. Clays are readily detected in the core but polyhalite (especially when not associated with iron oxide) may be difficult to detect and to visually estimate its quantity.

A correlation was found to exist between polyhalite content and the bromine content of the associated halite. This may not be true for all salt deposits and was found to be different by at least one worker (Adams, 1967) for the Salado Salt. Further work needs to be done to prove (or disprove) this relationship but if it does exist, a bromine profile may serve two purposes when studying a salt deposit for a

repository site. First, it could supplement X-ray diffraction and/or thin section analysis in detecting of polyhalite concentrations and potential dewatering zones. Second, it might indicate a proximity to other potash minerals which might represent zones of high water loss or areas of economic importance.

Unless current thinking about the composition of seawater and the partitioning of the bromine between halite and seawater is incorrect the bromine profile suggests that the Salado Salt is a second generation evaporite sequence, perhaps derived from preexisting halite brought in from surrounding areas or possibly recrystallized in place. Adams (1967, p. 163) prefers to think that the Salado was derived from older Permian and Pennsylvanian evaporites (of Arizona, Utah, Kansas, Oklahoma, Colorado, northern New Mexico and the Texas Panhandle) as tectonic activity raised these deposits and erosion produced brines which accumulated in southeastern New Mexico and west Texas. This conclusion would be difficult to prove. However, it is unlikely that the Wellington Formation contributed to this process since it was also found to be a second cycle evaporite with low bromine concentrations of only 30 to 40 ppm. No samples in the Salado were discovered to be appreciably lower in bromine than the Wellington which might have suggested that the Salado was a third cycle salt derived from the Wellington.

Finally, petrographic evidence obtained from the samples studied suggests that the deposition of the Salado Salt occurred in relatively shallow water. Hopper crystals were evident throughout samples from both cores. While hoppers may be deposited in quiet, deep water, it

is more likely that the excellent preservation observed was promoted by accumulation of hoppers in water depths measured in tens and hundreds of feet of water instead of thousands of feet. Also, the deposit was probably subaerially exposed at least part of the time. This conclusion is based on the presence of euhedral grains of halite embedded in a clay-silt matrix and bedded nodular anhydrite. The embedded halite appears similar to that formed in exposed salt flats, periodically subjected to influxes of terrigenous material. Nodular anhydrite is thought to represent nodules of gypsum formed near the surface which are dehydrated to form anhydrite as they are gradually buried under new sediments. Such deposition of nodular gypsum and other evaporites has been termed a sahbka facies (Kinsman, 1969, p. 834).

Adams (1967, p. 468-469) also concluded that at least part of the Salado Salt was deposited in shallow water (10-50 meters) based on three lines of evidence. The bromine profile shows sharp rises and falls which indicates nearly static evaporation of small amounts of brine. Many of the clay seams appear to have formed as residual accumulations from the dissolution of halite. Finally, he finds evidence of erosion at the top of many ore zones.

REFERENCES

REFERENCES

Adams, J. E., and Frenzel, H. N., 1950, Capitan barrier reef, Texas and New Mexico: Jour. of Geol., vol. 58, 53 pp.

Adams, S. A., 1967, Bromine in the Salado Formation, Carlsbad Potash District, New Mexico: (Ph.D. thesis) Harvard University, Cambridge, Mass., 202 pp.

Beane, R. E., and Popp, C. J., 1975, Chemical, mineralogical and thermogravimetric analyses of selected core samples from Carlsbad, New Mexico: Final Report for Union Carbide Nuclear Corp., Oak Ridge, Tenn., Subcontract No. 3673-3, supplement #3, 67 pp.

Bertin, E. P., 1970, Principles and practices of x-ray spectrometric analysis: Plenum Press, New York, 215 pp.

Borchert, H., and Muir, R. O., 1964, Salt deposits: the origin, metamorphism and deformation of evaporites: D. Van Nostrand Co. Ltd., London, 338 pp.

Boeke, H. E., 1908, Über das Kristallisationsschema der Chloride, Bromide, Jodide von Natrium, Kalium, und Magnesium, sowie uber das Vorkommen des Broms und das Fehlen von Jod in den Kalisalzlagerstätten (On the crystallization pattern of the chlorides, bromides and iodides of sodium, potassium and magnesium as well as the occurrence of bromine and the absence of iodine in the potash salt deposits): Zeitschr. Krist., u. Miner., vol. 45, p. 346-391.

Bradshaw, R. L., and McClain, W. C., 1971, Project salt vault: a demonstration of disposal of high-activity solidified waste in underground salt mines: Oak Ridge Nat. Lab. Report 4555, 360 pp.

Braitsch, O., 1971, Salt deposits: their origin and compositions: Springer-Verlag, New York-Heidelberg-Berlin, 297 pp.

Braitsch, O., and Herrmann, A. G., 1963, Zur Geochemie des Broms in salinaren Sedimenten, Teil I; Experimentelle Bestimmung der Br-Verteilung in verschiedenen naturlichen Salzsystemen (The geochemistry of bromine distribution in different natural salt systems): Geochim. et Cosmochim. Acta, vol. 27, p. 361-391.

Briggs, L. I., and Lucas, P. T., 1954, Mechanism of Salina Salt deposition in the Michigan Basin: Bull. Geol. Soc. of Amer., vol. 65, 23 pp.

Claiborne, H. C., and Gera, F., 1974, Potential containment failure mechanisms and their consequences at a radioactive waste repository in bedded salt in New Mexico: Oak Ridge Nat. Lab. Report TM-4639, 84 pp.

Clarke, F. W., 1924. The data of geochemistry: U. S. Geol. Sur. Bull., vol. 77, p. 220.

Committee on Radioactive Waste Management, 1970, Disposal of solid radioactive waste in bedded salt: National Academy of Sciences-National Research Council, Washington, D. C., 28 pp.

Dellwig, L. F., 1955, Origin of Salina Salt of Michigan: Jour. of Sed. Petrol., vol. 25, p. 89.

_____, 1968, Primary sedimentary structures of evaporites in Geology of saline deposits, Richter-Bernburg, G., ed., Unesco, 1972, 13 pp.

Fallis, S. M., 1973, Mineral sources of water and their influence on the safe disposal of radioactive waste in bedded salt deposits: (M. S. thesis) Univ. of Tennessee, Knoxville, 60 pp.

Hidalgo, R. V., and Renton, J. J., 1970, The use of pelletized samples for x-ray diffraction analysis of clay minerals in shale: West Virginia Geological and Economic Survey, circular 12.

Holser, W. T., 1966, Bromide geochemistry of salt rocks: Second Symposium on Salt, Northern Ohio Geological Society, Inc., vol. 2, 27 pp.

Jones, C. L., 1964, Petrography of evaporites from the Wellington Formation near Hutchinson, Kansas: U. S. Geol. Sur. Bull. 1201-A, 70 pp.

Kinsman, David J. J., 1969, Modes of formation, sedimentary associations, and diagnostic features of shallow-water and supratidal evaporites: Amer. Assoc. of Petrol. Geol. Bull., vol. 53, 10 pp.

Kopp, O. C., and Combs, D. W., 1975, Mineral sources of water in evaporite sequences (Salado Salt and adjacent beds at the proposed waste disposal facility near Carlsbad in Lea and Eddy Counties, New Mexico): Final Research Report for Union Carbide Nuclear Corp., Oak Ridge, Tenn., Subcontract No. 3670, supplements Nos. 3 & 4, 32 pp.

Kopp, O. C., and Fallis, S. M., 1973, Mineral sources of water in evaporite sequences: Final Research Report for Union Carbide Nuclear Corp., Oak Ridge, Tenn., Subcontract No. 3670, 40 pp.

Krauskopf, K. B., 1967, Introduction to geochemistry: McGraw-Hill Book Co., New York, 721 pp.

Kühn, R., 1955, Mineralogische Fragens der in den Kalisalzlagerstätten vorkommenden Salze, Kalium-Symposium (Internat. Kali-Inst., Bern), p. 51-105.

_____,1968, Combined evaluation of Br^- and Rb^+ contents for genetic characterization of carnallites and sylvite rocks in Geology of saline deposits, Richter-Bernburg, G., ed., Unesco, 1972, 13 pp.

Mason, B., and Berry, L. G., 1968, Elements of mineralogy: W. H. Freeman and Co., San Francisco, p. 364.

McClain, W. C., Lomenick, T. F., and Lowrie, R. S., 1975, Geologic disposal evaluation program: semiannual report (ending March 31, 1975): Oak Ridge Nat. Lab. Report 5052, 135 pp.

Nielsen, H., 1968, Sulfur isotopes and the formation of evaporite deposits in Geology of saline deposits, Richter-Bernburg, G., ed., Unesco, 1972, 12 pp.

Operator's Manual, 1974, Model 6110 and 6111 TEFA-Tube Excited Fluorescence Analyzer, ORTEC, 120 pp.

Pierce, W. G., and Rich, E. I., 1962, Summary of rock salt deposits in the United States as possible storage sites for radioactive waste materials: U. S. Geol. Sur. Bull. 1148, 91 pp.

Raup, O. B., 1970, Brine mixing: an additional mechanism for formation of basin evaporites: Amer. Assoc. of Petrol. Geol. Bull., vol. 54, #12, 12 pp.

Schaller, W. T., and Henderson, E. P., 1932, Mineralogy of drill cores from the potash field of New Mexico and Texas: U. S. Geol. Sur. Bull. 833, 120 pp.

Sloss, L. L., 1969, Evaporite deposition from layered solutions: Amer. Assoc. of Petrol. Geol. Bull., vol. 53, 10 pp.

Schmalz, R. F., 1969, Deep-water evaporite deposition: a genetic model: Amer. Assoc. of Petrol. Geol. Bull., vol. 53, 25 pp.

Valyashko, M. G., 1956, Geochemistry of bromine in the process of salt deposition and the use of the bromine as a genetic criterion: Geochemistry, vol. 6, 19 pp.

APPENDICES

APPENDIX A

BROMINE ANALYSES

The x-ray spectrograph employed for the final bromine analyses was an ORTEC 6110 TEFA (tube-excited fluorescence analyzer) made by ORTEC, Inc., of Oak Ridge, Tennessee. The 6110 TEFA proved to have distinct advantages in this study as compared with the Norelco Vacuum X-ray Spectrograph. While the basic principles of x-ray fluorescence spectroscopy are the same, this instrument incorporates a nondispersive, solid state detector which measures energy levels. The detector consists of a slice of silicon into which lithium has been diffused from one face. According to the ORTEC 6110 TEFA Operators Manual (1974), the wafer is a reverse-biased diode which permits current to flow when energy is absorbed and ionizes some of its atoms. The amplitude of the output current from the detector is directly proportional to the number of atoms ionized on the Si(Li) wafer by the fluorescing radiation from the sample. The detector and input stage of the preamplifier are operated at liquid nitrogen temperature (-195.8°C) to minimize lithium mobility and electronic noise. Instead of detecting the wavelength for a particular element (as in the Norelco X-ray Spectrograph) the ORTEC 6110 TEFA measures its energy levels in KeV. (Both methods are analogous because energy is inversely porportional to wavelength by the equation: $E = \frac{hc}{\lambda}$ where "h" and "c" are constants.)

The output from the detector is processed in a multichannel analyzer which accumulates an energy spectrum as a histogram composed

of up to 1024 channels. The display appears as peaks composed of small dots which rise above the baseline when energy is detected in a certain interval. This allows a rapid, semiquantitative scan for all elements present. A useful feature of the ORTEC instrument is that it permits the selection of a "range of interest" (ROI). The operator can select as many channels as desired to cover the number of counts accumulated for an entire peak (not just the position which is accumulating the largest number of counts as is done with the gonimeter of a typical x-ray spectrograph). The operator can then visually set background positions on both sides of the peak and determine that the instrument is not counting any abnormal low or high points.

The ORTEC 6110 TEFA is fully automated. It can be set for optimum conditions (anode current and voltage, filter type, etc.) while observing the display profile. With the standards and unknowns in place, the instrument can automatically analyze up to twelve samples for any number of desired elements which can be run under the same set of conditions. The computer then determines a linear and/or quadratic fit for the standards and compares the sample values against the standard curve(s). The final data is printed out in the units selected (ppm, µg/ml, percent) along with the number of counts per second.

The operating conditions for the bromine analyses were as follows:

Anode:	molybdenum	MCA:	40ev/channel
Kilovolts:	40	Digital gain:	1
Microamps:	50	Filter:	.005" molybdenum

Two additional elements (iron and chlorine) were also run but since no standards were available, arbitrary values of 1 ppm were used

for both elements. The data obtained (counts per second) permits relative estimates of the amount of these elements present. Iron content was analyzed since several potash minerals (sylvite and polyhalite) tend to have associated iron oxides. However, no conclusions were drawn from this data. Chlorine was analyzed in order to assure that the samples were relatively equal in content and that bromine concentrations would not be used taken from a sample that was grossly deficient in sodium chloride. All samples had values ranging between 60 to 65 cps and most had either 62 or 63 cps.

The computer printout for each analysis with the ppm values for bromine and cps values for iron and chlorine is stored for future reference at the Department of Geological Sciences, University of Tennessee, Knoxville.

APPENDIX B

MINERALOGY OF SELECTED SAMPLES OF THE SALADO SALT (AEC CORES #7 AND #8) BASED ON X-RAY DIFFRACTION ANALYSIS

Samples were run to determine the amount and kinds of minerals present. However, unless the mineral was present in amounts of 1 to 3 percent or more it was difficult to separate from the background. An approximate (semiquantitative) analysis was done in the following manner. A sample of the pure or nearly pure mineral (halite, polyhalite and anhydrite) was run on a scale of 2000 in order that no peak would go off the chart paper. From this, the height of the major peak for each mineral (halite-2.82 Å, polyhalite-2.92 Å, anhydrite-3.50 Å) was adjusted to 100 units (taking into account for the amount of other minerals present in the nearly pure samples). A mineral's abundance was determined by using the adjusted peak height. This is an approximate procedure which assumes an essentially linear fit between the peak height and the percentage of the mineral present and also assumes no constructive or destructive interference of the reflections between the minerals.

The approximate divisions for this study were major (M) constituents (>25 percent), minor (mi) constituents (5-25 percent) and trace (tr) constituents (<5 percent). No quantity was estimated for quartz, clays or magnesite. Their presence is denoted by an X in Table V. Other minerals were thought to be observed but could not conclusively be separated from the background.

TABLE V

MINEROLOGY OF CORE SECTIONS

Depth Meters	Depth Feet	Halite	Polyhalite	Anhydrite	Quartz	Clays	Magnesite
AEC #7							
318.2	1044	M		tr			
337.4	1107	M	M	M	X	X	
356.9	1171	M	mi	M			
372.2	1221	M	tr	tr	X		
395.0	1296	M	tr	tr	X		
409.0	1342	M	mi				
427.3	1402	M	tr				
447.4	1468	M	mi	tr	X	X	X
467.3	1533	M	mi				
492.3	1615	M	tr	tr			
517.2	1697	mi	M	M			
534.9	1755	M	tr	tr			
595.0	1952	M	mi	tr(?)			
595.6	1954	M	tr	tr	X	X	
596.8	1958	M	mi		X	X(?)	
597.4	1960	M	mi				
599.5	1967	M	mi				
600.2	1969	M	mi				
601.4	1973	M	mi				
602.0	1975	M	tr				
602.9	1978	M	mi			X	X
604.4	1983	M	mi	tr			
605.3	1986	M		tr			
607.5	1993	M	mi				
823.6	2702	M		tr			
827.8	2716	M		tr			
833.9	2736	M		tr			
AEC #8							
424.0	1391	M	tr				
455.7	1495	M	tr				
479.5	1573	M	tr	tr			
503.5	1652	mi	M	tr			
519.7	1705	M	mi	tr			
539.2	1769	M	tr				
544.7	1787	M	M				

TABLE V (continued)

Depth							
Meters	Feet	Halite	Polyhalite	Anhydrite	Quartz	Clays	Magnesite
546.8	1794	M	M		X	X	X
549.9	1804	M					
557.5	1829	M					
560.2	1838	M	mi	tr	X	X	
566.0	1857	M	tr				
571.5	1875	M		tr	X	X	X
574.2	1884	M	tr	tr	M	X	
576.1	1890	M	mi				
577.3	1894	M	tr		X	X	
578.8	1899	M	mi				
579.1	1900	M	mi	tr(?)			
580.6	1905	M	tr		X	X	X
582.5	1911	M	tr				
583.1	1913	M					
584.0	1916	M	mi				
586.1	1923	M	M			X	
588.3	1930	M	mi	tr		X	
589.2	1933	M	tr				
590.7	1938	M	mi				
595.3	1953	M	mi				
599.5	1967	M	mi	tr		X	X
605.3	1986	tr	M	tr	X		X
611.4	2006	M	mi	tr			
614.8	2017	M	mi	tr	X	X	X
621.5	2039	M	M	tr			
624.8	2050	M		M			tr
630.3	2068	M	tr	tr			
635.2	2084	M	mi	tr	X	X	
649.2	2130	M	tr	tr			X(?)
659.0	2162	M	mi		X		
675.7	2217	M	mi	tr			
694.9	2280	M	tr	tr(?)			
709.0	2326	M		tr		X	X
721.2	2366	tr	M	tr	X	X	X
739.7	2427	M		tr			
749.8	2460	M		tr			

A Norelco Diffractometer was used with a copper target at 35 kilovolts and 17 milliamps. The radiation was passed through a crystal monochromator to remove the CuK_β but to allow the CuK_α radiation to pass. All samples were run at a scale of 100 with a time constant of 2 seconds at a chart and goniometer speed of 1° 2θ per minute from 3° to 60° 2θ (29.4 Å to 1.5 Å).

APPENDIX C

PETROLOGY OF CORES AEC #7 AND #8

Abbreviations

Minerals. In the thin section descriptions the approximate amount of the minerals present are indicated by upper and lower case letters. Example: anhydrite; AN = MAJOR (>25 percent), An = Minor (5 to 25 percent), an = trace (<5 percent, often less than 1 or 2 percent).

AN	=	Anhydrite	GYP	=	Gypsum
CAR	=	Carnallite	HA	=	Halite
CEL	=	Celestite	KAIN	=	Kainite
CSSM	=	Clay and silt-sized minerals (often magnesitic)	MAG	=	Magnesite
			PH	=	Polyhalite
			QTZ	=	Quartz
FELD	=	Feldspar(s)	SYL	=	Sylvite
GLAU	=	Glauconite			

Other terms.

acic	acicular	incl	inclusion(s)
alg(lam)	algal (laminations)	iso	isolated
app	appear	lg	large
assoc	associated	macro	macroscopic (ally)
auth	authigenic	mg	medium-grained (1 mm to 1 cm)
bed	bedded	mat	material
cr bd	cross-bedded	nod	nodular
cg	coarse grained (>1 cm)	num	numerous
clus	cluster(s) of crystals	obs	observed
def	deformed	p	patches
dis	distinct(ive)	p&s	patches and stringers
env	environment	pet	petroliferous
ev	evidence	poss	possible
FeO	iron oxide(s)	pp	poorly preserved
fg	fine-grained (<1 mm)	pseudo	pseudomorph
flow	flowage	rad	radial
foss	fossil (iferous)	repl	replace(s) (ing)
fract	fracture(s)	repr	represent(s) (ing)
gr bd	grain boundary(ies)	sel	selvage(s)
HOP	hopper	s	stringer(s)
ig	intergrowth	sm	small

spher	spherulitic	tr	trace(s)
subaer	subaerial	tw	twinned
surr	surrounded by	w/	with
tab	tabular	xtal	crystal(s)
text	texture	(?)	questionable

Thin Section Descriptions

AEC-7

1044 cg HA; num fract, many filled by pet mat; tab An in cssm p and filling fract.

1107 fg to mg HA; gr bd and fract oft filled by pet mat; fg to prism to tab AN w/spher forms; poss gyp (?) w/sieve text fg Ph.

1171 App macro bed fg AN w/starburst (?); Ha ig between AN; fg Ph intermixing w/AN and forms starburst.

1221 cg HA; num fract; An in fg p&s and along fract; some radiating An forms; ph repl An.

1296 mg to cg HA; CSSM in p&s; poss some CSSM is ig; minor ph and an (?) in p&s.

1342 mg to cg HA; num fract; cssm and ph filling fract; tr an.

1402 mg to cg HA; prism Ph assoc w/fract; tr tab an.

1468 mg HA; CSSM w/ig cubic HA xtals (shallow water); qtz and feld (?) and mag (?) assoc w/CSSM; tr an and ph.

1533 cg HA w/HOP; num fract partly filled w/pet mat; Ph in p&s and along fract and ig; tr cssm.

1615 cg HA w/HOP; dis gr bd; p&s of fg Ph w/mg An; some mg An in p and iso.

1697 macro bed; mg An xtals set in fg PH; massive PH repl An; fg An (?) also; Ha ig and fills openings; tr syl and FeO and cssm.

1755 mg to cg HA w/HOP; num fract; Ph fract filling; tr an; some Ph repl an; tr syl.

1952 app macro bed mg to cg HA w/HOP; prism An xtals scattered; some ph repl An.

1954 cg HA; cssm w/qtz and feld in p&s (along fract); fg and acic ph assoc w/cssm and FeO; cssm cracked-dessication.

1958 mg to cg HA; dis gr bd; fg acic ph xtals in p&s; cssm in p&s w/qtz.

1960 poss macro bed (?); fg to cg HA w/HOP; cssm ig; fg ph ig; prism and tab an; qtz w/cssm.

1967 cg HA w/pp HOP; p&s of fg ph, some ig; tr prism an xtals; poss flow.

1969 fg to mg HA w/pp HOP; ig Cssm w/qtz and feld (?); mg an xtals, no assoc; tr ph.

1973 cg HA; minor fract but filled w/pet mat; tr an, cssm and ph (?).

1975 cg HA; p&s and fract filling of fg Ph with mg an xtals; Ph repl an; Ph assoc w/cssm and FeO.

1978 mg to cg HA; ig Cssm w/qtz and mag (?) surr cubic HA xtals (shallow water); fg Ph in p&s and flow mixed w/fg prism An xtals iso mg, prism An xtals.

1983 mg to cg HA w/HOP; num fract; fg Ph in p&s and flow w/poss mg an xtals; ph repl an; some mg prism an xtals iso along gr bd.

1986 cg HA; num fract; tr ph and an and cssm.

1993 cg HA w/HOP; fg Ph in p&s w/incl of mg tab An xtals; ph repl An.

2702 mg to cg HA; dis gr bd due to pet mat and incl; cssm in p&s; fg An in p&s w/cssm.

2716 mg to cg HA w/HOP; fg An in p&s along fract; cssm present.

2736 mg to cg HA w/HOP; fg An in p&s along fract; cssm present.

AEC #8

1391 cg HA; fg ph in sel; fg an (?) in p&s, FeO.

1495 mg to cg HA w/HOP; fg Ph in p&s and lg; Ph assoc w/CSSM and shows ev of flowage.

1573 macro app bed; mg to cg HA; fg Ph and fg to mg An in p w/sel; Ph repl An repl nod gyp (?); car (?).

1652 macro app bed; slide divided into two dis text halves; one-half fg An w/l An xtals; other half fg to mg Ph and An; mg Ha in P; fg syl; poss lg lam in An.

1705 fg to cg HA w/HOP; fg Ph in p&s and ig oft assoc w/an at gr bd; FeO.

1769 mg to cg HA w/pp HOP; fg to mg Ph in p&s and ig; Ph repl HA; fg gyp (?) dis "swallow tail" tw; poss cel, acic (?); FeO.

1787 mg to cg HA w/HOP; Ph in p&s and ig; l an xtals; poss flowage; acic cel (?); fg to mg gyp (?).

1794 macro bed; fg to mg HA w/HOP; fg CSSM; HA ig in CSSM-FeO matrix, primary depositional feature; iso ph xtals; auth qtz and feld, w/tr glauc (?).

1804 fg to cg HA w/pp HOP; fg CSSM-FeO in ig; few cg an and acic ph xtals in ig CSSM, also clusters of ph.

1829 cg HA w/HOP; numerous fl incl; right angle fract; ig Cssm-FeO tr ph.

1838 fg to mg HA w/pp HOP; dis gr bd; Cssm ig w/HA; an p and fg acic Ph assoc w/Cssm-FeO.

1857 cg HA w/pp HOP; tr ph along is.

1875 macro bed; fg to mg HA ig in CSSM matrix (subaerial type deposit) iso xtal and p of ph and fg to mg an; auth qtz and feld; FeO.

1884 fg to mg HA w/HOP; CSSM and FeO; iso and clusters of fg to mg an (poss pseudo after gyp) tr syl; some fracture filling by an.

1890 mg to cg HA w/HOP; some fract; ig ph and fract filling; some fg an in p.

1894 mg to cg HA w/pp HOP; numerous incl marking dist gr bd; fg ph and an in p&s; acic an along gr bd; cssm in p&s w/auth qtz and feld.

1899 fg to cg HA w/HOP; ig Cssm; tr an and ph; oft iso.

1900 fg to cg HA w/HOP; fract and flowage; fg p of ph w/an xtals; ev of ph repl an; ig cssm.

1905 mg to cg HA w/l ig p Cssm; cracks in cssm filled by second generation HA; tr ph and an; qtz.

1910 mg to cg HA w/pp HOP; healed fract; ig and p&s Ph and an and cssm; Ph app to repl an.

1911 mg to cg HA w/HOP; p&s of Ph and An; Ph and some cssm in ig; Ph repl an.

1913 fg to cg HA w/ig Cssm and Cssm incl in HA; tr acic ph; auth qtz and feld.

1916 cg HA w/pp HOP; p&s of ph mixed w/mg an along fract.

1923 (two slides) fg to cg HA; cubic xtals of HA in Cssm matrix (mud-flat environ.); iso and p&s of ph and an; auth feld.

1930 mg to cg HA w/pp HOP; dis gr bd; acic ig Ph and an; also p&s of Ph and an fg; tr cssm; gyp (?).

1933 cg HA w/HOP; ig petilliferous material; p&s of cssm and ph and an; sel oft around ph; auth qtz and feld.

1938 cg HA w/pp HOP; p&s of an and ph w/sel and mg iso ph xtals.

1953 fg to mg Ha w/l HOP; dis gr bd; p&s and iso xtals of acic an surr by fg ph in s and gr bd.

1967 fg to cg Ha w/HOP; ig p&s and fract filling of Cssm w/auth qtz and feld; scattered Ph and An.

1986 app cr-bed; PH and AN ig w/cssm; AN mg and PH fg; PH repl AN; some AN pseudo after gyp (?); alg lam present (?).

2006 fg to cg HA w/HOP; p&s of an and Ph (assoc FeO); Ph repl an; tr syl; numerous incl marking gr bd.

2017 mg to cg HA w/HOP; few fract and incl; Ph repl an w/sel surr Ph; p of cssm; mag grains (?).

2039 mg to cg HA w/HOP; p&s of Ph and an w/cssm; Ph oft radial; Ph repl an.

2050 mg AN; numerous incl; Ha ig; few fract; cssm w/FeO.

2068 fg to cg HA; p&s of cssm assoc w/fract oft; p&s of An and ph (?); an pseudo after gyp (?) as ev by form.

2084 fg to cg HA; many fract; many p&s of Cssm and FeO; HA xtals growing in Cssm matrix; p&s and fract fillig of Ph in acic form.

2130 fg to mg HA; dist gr bd; cssm present; ig An w/sel of ph (?); no FeO; An fg to mg and sometimes along fractures.

2162 cg HA; ig p of Ph and Cssm and FeO; Ph surr by sel w/tr of an; poss syl (?).

2217 cg HA; fract and few incl; p&s of Ph and an; some Ph rad and repl an; some Ph and an along fract; syl (?) assoc with Ph starburst.

2280 fg to cg HA; dis gr bd because of incl; fg Ph and an in p and fract assoc w/cssm; kainite (?).

2326 fg to cg HA w/pp HOP; cubic HA xtals in Cssm matrix (shallow water feature); iso xtals of an and ph; mag cssm w/auth feld (?).

2366 poss macro bed; PH dominate in rad starburst; some an, qtz, cssm.

2427 fg to cg HA w/pp HOP and fract; fg An w/1 xtal incl; cssm and some an ig.

2460 mg to cg HA w/HOP; fract obs; gr bd dist; p&s of fg An and cssm and qtz.

2519 mg to cg HA w/pp HOP; p&s and ig fg an oft assoc w/cssm.

2563 poss bed; nodular masses fg AN surr some mg AN; Cssm in p w/poss mud crack or burrowing (?).

2616 fg to mg HA w/pp HOP; gr bd dis; ig and p&S of An and cssm; fract.

2666 fg to cg HA w/pp HOP and many fract; p&s of fg an and cssm assoc.

2707 cg HA w/HOP; p&s of an and cssm.

2758 fg to mg HA w/pp HOP; dis gr bd; fg p of An and iso xtals; some cssm assoc An; many fract.

2779 mg to cg HA w/pp HOP; dis gr bd. p&s of fg to mg An and Cssm.

2793 fg to cg HA w/pp HOP; fg An assoc w/fract and cssm in p&s; poss tr of ph (?); poss qtz and mag.

2803 fg to cg HA w/HOP; p&s of fg HA; An in p w/some larger An xtals; cssm and fract.

2809 mg HA w/pp HOP; gr bd not dist; p&s of An and cssm w/sel surr An; poss tr ph (?).

2821 mg to cg HA w/HOP; p of incl; ig and p&s of fg An and cssm.

2879 poss macro bed; fg to mg HA w/HOP; p&s of An in HA xtals; some iso xtals of poss ph (?).

2948 poss macro bed; mg to cg HA w/HOP; dist gr bd; nod p (banded) An and some iso xtals.

APPENDIX D

PLATES

Plate 1. Halite hopper crystal.

Fossil hopper crystal outlined by inclusions along crystal faces. Many times only one intersection of the faces is observed and gives the appearance of "chevrons."

Plate 2. Fracture-filling of halite.

A fracture in halite filled by polyhalite (white) and clays (dark). Notice numerous fractures in halite along edges of thin section.

Plate 1

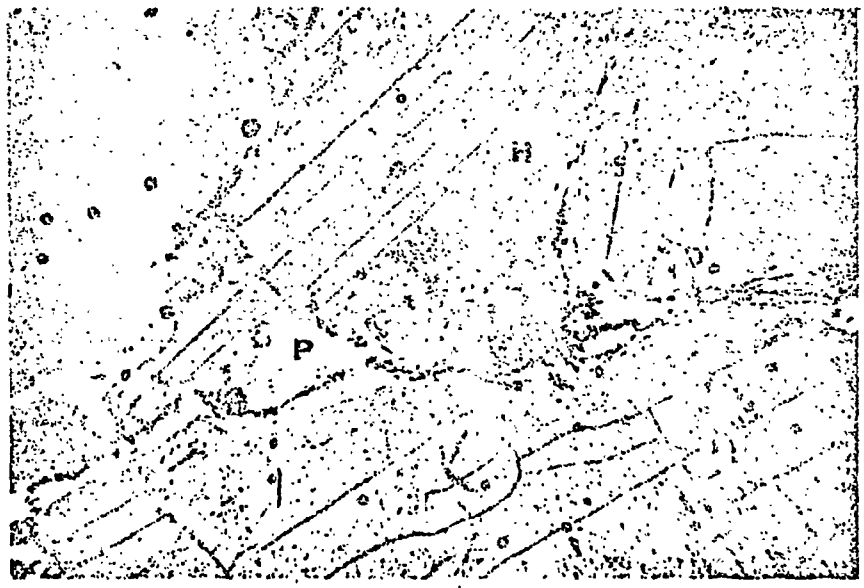

Plate 2

Plate 3. Possible deformation resulting in flowage of polyhalite.

Massive, fine-grained polyhalite appears to be deformed and almost be in a state of flowage.

Plate 4. Polyhalite starburst.

Spherulitic habit shown by polyhalite. Acicular crystals radiate from a common point, often a seed crystal.

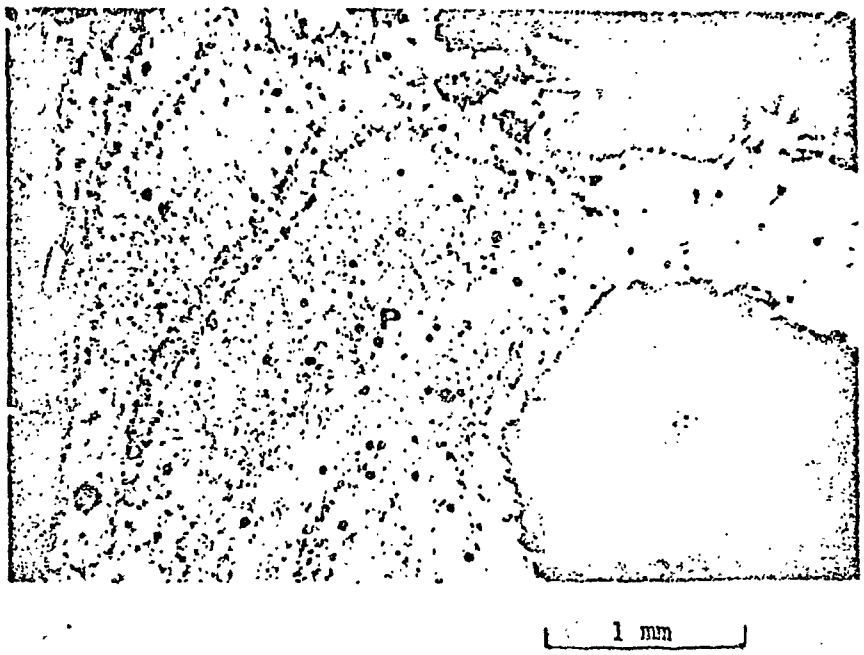

Plate 3

Plate 4

Plate 5. Fine-grained polyhalite replacing coarse-grained anyhdrite.

Large crystals of anhydrite are often replaced by a fine-grained polyhalite. Notice the serrated edges of the anhydrite especially on the end of the elongated anhydrite crystal.

Plate 6. Euhedral halite grains embedded in clay matrix.

Well-developed halite grains embedded in a clay matrix are observed in several thin sections and thought to represent a shallow-water feature. Small grains (white) in clay (dark) are primarily quartz and feldspars.

165 microns

Plate 5

1 mm

Plate 6

Plate 7. Sylvite grains in halite.

Isotropic wylvite in halite matrix. Shaded areas are associated iron oxide staining. Notice the disseminated clays throughout the halite.

Plate 8. Dessication cracks in clays.

"Mud cracks" in clays. Whether these formed on the surface in the usual manner or just from the dessication of a buried clay is unknown.

0.2 mm

Plate 7

1 mm

Plate 8

Douglas W. Combs [redacted]

In 1968 he entered the University of Tennessee at Knoxville and after a short intermission for military service, he received a Bachelor of Science degree in geology in 1973. Continuing in the Master's program at the University of Tennessee, he was chosen as a research assistant for a project under a subcontract with Union Carbide Nuclear Corporation, Oak Ridge, Tennessee and graduated in 1975. This project formed the basis for this thesis.

He has accepted a position with the Fossil Fuels Branch of the Tennessee Valley Authority in Chattanooga.